

Annual Review of Earth and Planetary Sciences

Modeling Past Hothouse Climates as a Means for Assessing Earth System Models and Improving the Understanding of Warm Climates

Jiang Zhu,¹ Christopher J. Poulsen,² and Bette L. Otto-Bliesner¹

Annu. Rev. Earth Planet. Sci. 2024. 52:12.1-12.28

The Annual Review of Earth and Planetary Sciences is online at earth.annualreviews.org

https://doi.org/10.1146/annurev-earth-032320-100333

Copyright © 2024 by the author(s). All rights reserved

Keywords

hothouse climate, early Eocene, surface temperature, Earth system model, physical parameterization, model assessment and improvement

Abstract

Simulating the warmth and equability of past hothouse climates has been a challenge since the inception of paleoclimate modeling. The newest generation of Earth system models (ESMs) has shown substantial improvements in the ability to simulate the early Eocene global mean surface temperature (GMST) and equator-to-pole gradient. Results using the Community Earth System Model suggest that parameterizations of atmospheric radiation, convection, and clouds largely determine the Eocene GMST and are responsible for improvements in the new ESMs, but they have less direct influence on the equator-to-pole temperature gradient. ESMs still have difficulty simulating some regional and seasonal temperatures, although improved data reconstructions of chronology, spatial coverage, and seasonal resolution are needed for more robust model assessment. Looking forward, key processes including radiation and clouds need to be benchmarked and

¹Climate and Global Dynamics Laboratory, National Center for Atmospheric Research, Boulder, Colorado, USA; email: jiangzhu@ucar.edu

²Department of Earth Sciences, University of Oregon, Eugene, Oregon, USA; email: poulsenc@uoregon.edu

improved using more accurate models of limited domain/physics. Earth system processes need to be better explored, leveraging the increasing ESM resolution and complexity.

- Earth system models (ESMs) are now able to simulate the large-scale features of the early
- Remaining model-data discrepancies exist at regional and seasonal scales and require improvements in both proxy data and ESMs.
- A hierarchical modeling approach is needed to ensure relevant physical processes are parameterized reasonably well in ESMs.
- Future work is needed to leverage the continuously increasing resolution and complexity of ESMs.

1. BACKGROUND

Past climates inform our future (Tierney et al. 2020). They provide exploration of climate states outside of the narrow range of the recent historical period. Through comparison with climate proxy data from the geologic record, paleoclimate reconstructions of past hothouse climates (Westerhold et al. 2020) can be used to assess the performance of Earth system models (ESMs) and to improve the understanding and modeling of future warming climates. As noted by the pioneering paleoclimatologist John E. Kutzbach, "climate forecasts suffer from lack of accountability. Their moment of truth is decades in the future. But when those same computer programs are used to hindcast the past, scientists know what the correct answer to the test should be."

One of the most persistent and challenging tests that ESMs have faced is simulating the very warm surface temperatures and the low equator-to-pole temperature gradient of past hothouse climates, most notably the mid-Cretaceous and the early Eocene, a shortcoming that has been termed the equable climate problem (Barron 1983, 1987). The mismatch between model and proxy data highlights the progress still needed for ESMs to simulate climate dynamics under extreme warm conditions and raises important questions about their ability to accurately project future anthropogenic warming. The causes of the model-data discrepancy have been the focus of considerable attention. Early studies focused on the possible reorganization of atmospheric and oceanic circulations to provide the implied higher meridional heat transport (Covey & Barron 1988, Farrell 1990), which was later found to be challenging to reconcile with coupled ocean-atmosphere model simulations (Bush & Philander 1997, Huber & Sloan 2001, Otto-Bliesner et al. 2002). Later investigations could be broadly grouped into three categories, focusing on (a) uncertainty in the reconstructions of the paleoclimate environment that are used for model boundary conditions, (b) the misrepresentation or absence of fundamental physical or Earth system processes in ESMs, and (c) incorrect or uncertain interpretations of proxy data. Below, we briefly summarize some of these issues.

With regard to model boundary conditions, past modeling studies have implicated paleogeography, including the position of continents, opening of ocean gateways, and height of mountain ranges, as important factors influencing warmth during past geological timescales (Barron & Washington 1984, Norris et al. 1999, Poulsen & Zhou 2013, Poulsen et al. 2003, Shellito et al. 2009). While climatically important at regional scales, these factors have not been shown to independently account for the global warmth of past hothouse climates. Higher CO₂ concentrations in the atmosphere have been considered a key ingredient for explaining the global warmth of hothouse climates (Barron & Washington 1985). However, until recently, model predictions based on proxy best estimates of CO₂ did not produce enough warming (Caballero &

Hothouse climate: extreme warm climate with ice-free poles and a global mean surface temperature usually more than 10°C higher than today's

Climate dynamics: principles governing the thermal, radiative, and dynamical processes of the atmosphere and ocean and their interactions with the other Earth components

Huber 2013), leading to searches for other explanations for warmth. Non-CO₂ greenhouse gases (GHGs) (Beerling et al. 2011, Bice et al. 2006) and oxygen levels (Poulsen et al. 2015) have also been suggested as contributors, although these factors are much less constrained by proxy data.

The misrepresentation or absence of processes in ESMs generally concerns both the model complexity and the ability to represent physical processes at the model resolution. As an example of the former, early ESMs did not predict vegetation type and phenology changes and thus may have missed a mechanism to warm global and regional temperatures (Otto-Bliesner & Upchurch 1997). Likewise, the absence in ESMs of a link between biological productivity and aerosol abundances has been hypothesized to be a missing complexity for explaining the warm and equable climate (Kiehl & Shields 2013, Kump & Pollard 2008). Similarly, polar stratospheric clouds that depend on the model capabilities of interactive atmospheric chemistry and stratospheric dynamics have also been hypothesized to be the missing element for producing high-latitude surface warming (Dutta et al. 2023, Kirk-Davidoff et al. 2002, Sloan & Pollard 1998).

The representation of physical processes at a typical ESM grid (usually with coarse horizontal grid spacing greater than ~100 km) has been a continuous theme in past investigations of the equable climate problem. At coarse resolution, ESMs cannot resolve atmospheric convection and clouds, oceanic eddies, and turbulence in both systems; their effects on the simulated climate have to be parameterized based on, oftentimes, incomplete physical understanding and observation (see the sidebar titled Model Parameterizations). Many past studies have focused on these atmospheric and oceanic processes that may be inadequately represented by model parameterizations. The initiation of polar atmospheric convection has been hypothesized to act as positive feedback to warm the surface and lead to an ice-free Arctic winter (Abbot & Tziperman 2008). Subsequently, the warm Arctic air can lead to formation of low clouds that can help to maintain a frost-free winter in the continental interior, as the warm maritime air moves inland (Cronin & Tziperman 2015). In a large-eddy simulation that explicitly resolves atmospheric boundary-layer turbulence over a limited domain, Schneider et al. (2019) reported an abrupt breakup of subtropical stratocumulus

MODEL PARAMETERIZATIONS

In modeling, to parameterize is to reduce a complex process into simpler, tractable terms. Parameterizations are an essential part of Earth system modeling; they exist everywhere in the model from evaporation of moisture at Earth's surface and the formation of clouds to where the wind carries the clouds and where and what type of precipitation eventually falls. Parameterizations are needed due to either the large computational demand or the lack of physical understanding of the relevant processes. As a result, parameterizations are approximate, either because of numerical cost issues (limitations in grid resolution, acceleration of radiative transfer computation) or, more fundamentally, because they summarize complex and multiscale processes through an idealized and simplified representation. With a horizontal grid size of ~100 km, Earth system models (ESMs) can resolve large-scale processes such as monsoon circulation and ocean gyres but are incapable of capturing fine-scale processes in the system, such as atmospheric boundary-layer turbulence, convection, clouds, precipitation, ocean mixing, and eddies. Parameterizations are designed to approximate the average effects of the subgrid-scale processes on an individual grid cell, using basic physical understanding, conceptual model, or empirical formulations derived from observation or high-resolution calculations. Parameterizations are responsible for most of the intermodel differences between ESMs. Often, newer parameterization schemes have more physical basis and are more complex, i.e., may have more underconstrained parameters. Parameterizations will exist in ESMs for the foreseeable future. Parameterizations that are mentioned in this review include those for radiation, boundary-layer moist turbulence and clouds, cloud microphysics and ice nucleation, and ocean eddies (see the sidebars in this article for details). General references for further reading are Morrison et al. (2020), Pincus et al. (2019), and Hewitt et al. (2022).

decks under warming and suggested the modeling of boundary-layer clouds and their interaction with thermodynamics and radiation as a key for warm climates. The important role of atmospheric convection and clouds has also been demonstrated in ESMs with different complexities. Using a perturbed-physics ensemble in a relatively simple ESM, Sagoo et al. (2013) found that the warmest members that compared best with proxy data had the lowest cloud cover and exhibited a reduction in the ratio of low to high clouds, although the exact reasons for these changes could not be identified. More recently, updated cloud schemes in the Community Earth System Model (CESM) version 1.2, a comprehensive ESM, were identified to be the key for capturing the extreme warmth and reduced equator-to-pole gradient of the early Eocene due to a reduction in cloud coverage and opacity (Zhu et al. 2019). Similarly to the atmospheric processes, representation of ocean subgridscale processes such as eddies (Nooteboom et al. 2022) and mixing, due to either tropical cyclones (Emanuel 2002, Korty et al. 2008) or tides (Green & Huber 2013), has also been hypothesized to explain discrepancies between model simulations and proxy data.

Like the models, proxy temperature methods and estimates have evolved and are associated with their own limitations and uncertainties. In fact, the original equable climate problem has been ameliorated by newer estimates of sea-surface temperatures (SSTs), especially in the tropics (Huber 2008). Early oxygen isotope records suggested that the tropical SSTs of the mid-Cretaceous and early Eocene were comparable to or colder than the present day (e.g., Shackleton & Boersma 1981). Recent efforts using records with better preservation and multiple proxies have increased the median estimation to 33-37°C (Bice et al. 2006, Evans et al. 2018, Hollis et al. 2019, Inglis et al. 2015, O'Brien et al. 2017, Pearson et al. 2001, Tripati et al. 2003, Wilson et al. 2002). The revision of tropical SSTs confirms a partial explanation of the equable climate problem that SST reconstructions have potential biases due to diagenesis (Schrag 1999), seawater isotope composition (Poulsen et al. 1999, Zachos et al. 1994), and calibration (Bernard et al. 2017, Ho & Laepple 2016), among other factors. While the revision has led to improved model-data comparison for these warm periods, challenges remain. For example, until recently, ESMs required extremely (and unreasonably) high levels of atmospheric CO2 to simulate proxy-suggested large-scale temperatures with various degrees of difficulties in capturing the low equator-to-pole gradient (Caballero & Huber 2013, Huber & Caballero 2011, Lunt et al. 2012, Poulsen & Zhou 2013, Tabor et al. 2016). On the regional and seasonal scale, temperature records over the high latitudes, such as the SST estimates from the Southern Ocean and the warm winter temperature and reduced seasonality in the continental interior, have been challenging for ESMs but proxy results are found to depend on the reconstruction method (Greenwood & Wing 1995, Hollis et al. 2012, Huber et al. 2018, Inglis et al. 2015, Korasidis et al. 2022, O'Connor et al. 2019, Reichgelt et al. 2022, Suan et al. 2017, West et al. 2020).

Proxy CO₂ reconstructions are in general more uncertain than temperature in Earth's deep past. The mid-Cretaceous and early Eocene values depend on proxy type and vary greatly among studies (Foster et al. 2017, Hollis et al. 2019). Boron-based marine reconstructions of the early Eocene CO₂ concentration range from 1,170 to 2,490 ppm* [upper and lower bounds of the 95% confidence intervals (CIs) from two methods] (Anagnostou et al. 2020; see also Rae et al. 2021), which is approximately 4-9× the preindustrial CO₂ (PIC) level (284.7 ppm*). Terrestrial CO₂ reconstructions are mostly lower than the marine-based values, which is likely related to the potential proxy saturation or large proxy uncertainty at very high CO₂ levels (e.g., Hollis et al. 2019).

Given the importance of the hothouse climate for understanding and constraining climate models, recent efforts have been made to compare multiple model simulations of the early Eocene and provide a global compilation of proxy data. The Eocene Modelling Intercomparison Project (EoMIP) provides an intercomparison of four models with early Eocene simulations that varied in their complexity and forcings (Lunt et al. 2012). The Deep-Time Model Intercomparison Project

(DeepMIP) built on the design of the EoMIP, with the experimental design specifying common paleogeography, GHGs, astronomical configuration, solar constant, land-surface processes, and aerosols as well as initial conditions within the models, to allow for a straightforward comparison of simulations (Lunt et al. 2017, 2020). One of the most significant outcomes of DeepMIP is the confirmation that Eocene global mean warming [relative to the preindustrial (PI)] arises primarily from the greenhouse effect due to enhanced CO₂ levels (Lunt et al. 2020). This conclusion supports the use of paleoclimates to provide insights into a future high-CO2 world. And, indeed, the Eocene appeared prominently in the Sixth Assessment Report (AR6) from the Intergovernmental Panel on Climate Change (IPCC) because of the overlap of long-term CO₂ estimations with the range projected for the end of the twenty-second century under the Shared Socioeconomic Pathways (SSPs) 5-8.5 scenario, i.e., CO₂ exceeding 1,000 ppm+ by 2100 and reaching 2,100 ppm+ by 2200 (IPCC 2021).

This review aims to provide perspectives on recent developments and important issues remaining for a robust mechanistic understanding and modeling of extreme warm paleoclimates. (For a comprehensive review of the modeling of hothouse climates using ESMs, readers are referred to Huber & Caballero 2011 and Lunt et al. 2020, 2012.) Here, we focus on the early Eocene hothouse climate because of the greater availability of both model runs and proxy constraints for this most recent hothouse period (Westerhold et al. 2020) and due to its prominence in the IPCC AR6.

2. DATA, METHOD, AND SIMULATIONS

2.1. Surface Temperature Records and Estimation of Global Mean Surface Temperature and Meridional Sea-Surface Temperature Gradient

We use the surface temperature compilation of the Early Eocene Climate Optimum (EECO; 53.26–49.14 Ma) (Hollis et al. 2019), which represents a comprehensive and consistent synthesis of the mean annual surface temperatures over the land and ocean. In addition, we include new terrestrial temperature reconstructions to increase the spatial coverage (Reichgelt et al. 2022, van Dijk et al. 2020), although these records may not strictly fall within the DeepMIP definition of EECO due to the lack of good age control. Recrystallized foraminifer δ^{18} O and paleosol records are not included, as they may suffer from a cool bias (Hollis et al. 2019, Inglis et al. 2020).

We estimate GMST of the EECO to be $28.3 \pm 2.5^{\circ}$ C (95% CI), following the method documented by Zhu et al. (2019) using the updated surface temperatures. The estimation is larger by 1.3°C than in a recent study, reflecting the dependence on methods and data sets (Inglis et al. 2020). In our method, GMSTs are first estimated for the land and ocean separately and then averaged by their area weights, which ensures that the result is not dominated by the larger number of terrestrial records (81 terrestrial versus 26 marine records). In addition, our method attempts to reduce the bias from the uneven spatial sampling of records (specifically the greater number of extratropical records) by averaging GMSTs calculated from absolute temperatures and temperature anomalies relative to the PI. The rationale is that using absolute temperature tends to underestimate the GMST due to the higher number (and lower temperature) of records from the extratropics, while using temperature anomalies tends to overestimate GMST due to the higher number (and higher anomalous temperature) of extratropical records. The PI temperatures are from the Berkeley Earth Land/Ocean Temperature Record (Rohde & Hausfather 2020). For details of the method including the uncertainty estimation, readers are referred to Zhu et al. (2019).

Similarly, we recalculated the meridional SST gradient (Δ SSTm) of the EECO using the method in Zhu et al. (2019), which is computed as the average tropical SST (30°S-30°N) minus the average polar SST (poleward of 60°S/N). The EECO deep ocean temperature is used as a substitute for the polar SST due to the scarce records over the polar region. EECO Δ SSTm,

Equilibrium climate sensitivity (ECS): the global mean surface air temperature increase that follows a doubling of atmospheric carbon dioxide

in percentage of the PI Δ SSTm, is estimated to be 72% with a 95% CI of 51–89%. The range is larger than that of Zhu et al. (2019), primarily due to the inclusion of recent clumped isotope reconstructions of EECO deep ocean temperatures that are warmer and more variable than the previous isotope- and Mg/Ca-based estimates (Cramer et al. 2011, Meckler et al. 2022, Westerhold et al. 2020).

2.2. Model and Simulations

The CESM series are state-of-the-art ESMs that explicitly represent the atmosphere, ocean, land surface, and sea ice, and the interactions between them, and have participated in multiple phases of the Coupled Model Intercomparison Project (CMIP) and the Paleoclimate Modelling Intercomparison Project (PMIP). The recent three versions of CESMs are the Community Climate System Model version 4 (CCSM4), CESM1, and CESM2 (Danabasoglu et al. 2020, Gent et al. 2011, Hurrell et al. 2013). Equilibrium climate sensitivity (ECS) increases from 3.2°C in CCSM4 to 4.2°C in CESM1 and to 6.1°C in CESM2, as calculated in slab ocean simulations under PI conditions with an ~2° atmosphere and land. The primary model difference that has the largest impact on ECS is the atmosphere component, which features the Community Atmosphere Model versions 4, 5, and 6 (CAM4, CAM5, CAM6, respectively) (Gettelman et al. 2012, 2019; Zhu et al. 2022).

CAM4, 5, and 6 differ in their radiation and cloud-related parameterizations (see the sidebars titled Parameterization of Radiation, Parameterization of Boundary-Layer Moist Turbulence and Clouds, and Parameterization of Cloud Microphysics and Ice Nucleation). CAM5 has updates from CAM4 in the physical parameterizations of radiation, boundary layer and shallow convection, aerosol, and cloud microphysics and macrophysics (Hurrell et al. 2013). CAM6 has updates from CAM5 including a new higher-order turbulence closure scheme with a unified description of processes in the cloudy turbulent layers, changes to the two-moment stratiform microphysics scheme including a new capability to predict the mass and number concentration of rain and snow, and modifications of the mixed-phase ice nucleation scheme (Gettelman et al. 2019). Due to these changes in physical parameterizations, CAM has made progressive improvements in cloud simulation when compared with satellite observations (Gettelman et al. 2019, Kay et al. 2012). Importantly, these radiation and cloud updates are also responsible for major differences in their simulation of past cold and hothouse climates (Zhu et al. 2019, 2021, 2022).

PARAMETERIZATION OF RADIATION

Radiation calculation is a fundamental part of climate modeling, as it computes the transmission of the shortwave (solar) and longwave (emission) radiation through the atmosphere that ultimately drives all atmospheric motions. Radiation must be parameterized in ESMs due to the enormous computational cost to explicitly resolve the spectral radiance and transmittance over the full spectral range. One common technique to parameterize the computation is to group optically similar spectral regions (i.e., wavelengths) together to reduce the number of calculations. The radiation parameterizations, e.g., the CAMRT (Community Atmosphere Model radiative transfer code) in CAM4, RRTMG [Rapid Radiative Transfer Method for GCMs (general circulation models)] in CAM5 and CAM6, and updated RTE+RRTMGP (Radiative Transfer for Energetics + Rapid Radiative Transfer Model for General circulation model applications—Parallel), differ in how they accomplish this. To further speed up the calculation, RRTMG and RTE+RRTMGP use precomputed lookup tables for gas absorption coefficients. The lookup table in the new RTE+RRTMGP is designed to cover broader climate conditions than in RRTMG. The accuracy of the radiation parameterization can be assessed using the sophisticated line-by-line (LBL) calculation that explicitly computes the spectral radiance and transmittance.

PARAMETERIZATION OF BOUNDARY-LAYER MOIST TURBULENCE AND CLOUDS

Turbulent updrafts in the atmospheric boundary layer (BL), the lowest part of the atmosphere that is directly impacted by Earth's surface, have a spatial scale of 10–100 m and are critical for the formation of low clouds that regulate Earth's radiation budget by shading the surface. The parameterization in ESMs describes the effects of small-scale processes on the model-resolved grids and in general involves providing closure assumptions for moist turbulence and/or convection and their interaction with the environment. The closure assumptions are usually derived from observation, conceptual models, or the large-eddy simulation that resolves the small-scale processes in a limited area. Newer schemes typically feature greater complexity and computational demand. For example, CAM4's scheme uses a simple, empirical profile of eddy diffusivity as the turbulence closure and does not include direct interaction between turbulence and moisture condensation. CAM5's scheme is formulated using moist thermodynamics and diagnoses the eddy diffusivity from the turbulent kinetic energy. CAM6's scheme uses a more advanced, high-order turbulence closure and provides a unified framework to provide consistent treatment of BL moist turbulence and clouds.

In this study, we focus mostly on the early Eocene simulations using the three CESMs for three reasons. First, CESM1 has been found to be one of the best ESMs for reproducing the early Eocene global mean warmth (GMST), large-scale \triangle SSTm, and hydrological cycle reconstructed in the geological record (Cramwinckel et al. 2023, Lunt et al. 2020, Zhu et al. 2019). Second, CESM2, CESM1, and CCSM4 have distinct physical parameterizations and cover a very wide range of GMST, essentially bracketing results from all the DeepMIP models (**Figure 1***a*). Third, the CESM framework is flexible and allows us to explore contributions from different radiation and cloud parameterizations to highlight their influences on the simulation of hothouse climate.

PARAMETERIZATION OF CLOUD MICROPHYSICS AND ICE NUCLEATION

Typical sizes of cloud and rain droplets are 20 and 2,000 micrometers (10^{-6} m) in diameter, respectively. Cloud microphysics describes a range of processes on this small scale (from submicrometer to centimeter) that drive the formation and evolution of cloud and precipitation particles, such as nucleation, condensation, collision and coalescence, evaporation, freezing, and melting. Cloud microphysical properties (particle mass, number concentration, and size, as well as phase of the condensates) intrinsically determine the radiative effects of clouds and precipitation. ESMs use bulk microphysical schemes with different complexities to model the population statistics of cloud microphysical properties, as tracking every cloud or precipitation particle individually is computationally prohibitive. For example, CAM4 uses a bulk one-moment scheme that predicts mass mixing ratios of cloud condensates. CAM5 uses a bulk two-moment scheme that predicts both the mass mixing ratios and the number concentration of cloud condensates, which allows for modeling the impact of aerosols on clouds and hence radiation. CAM6 microphysics updates the CAM5 scheme by predicting rather than diagnosing the mass and number concentration of rain and snow.

Parameterization of ice nucleation describes how cloud ice is formed [either homogeneously through cooling at cold temperatures (less than -38° C) or heterogeneously through interaction with aerosols]. Ice nucleation impacts climate through its influence on precipitation formation and the reflectivity and lifetime of clouds. CAM4 has no ice nucleation process, and the cloud ice and liquid partition is a linear function of temperature. CAM5 includes ice nucleation using an observation-based relationship as a function of temperature and supersaturation with respect to ice and does not directly connect with ice-nucleating aerosols. The CAM6 scheme takes advantage of classical nucleation theory and laboratory measurements and has built-in dependence on aerosol properties.

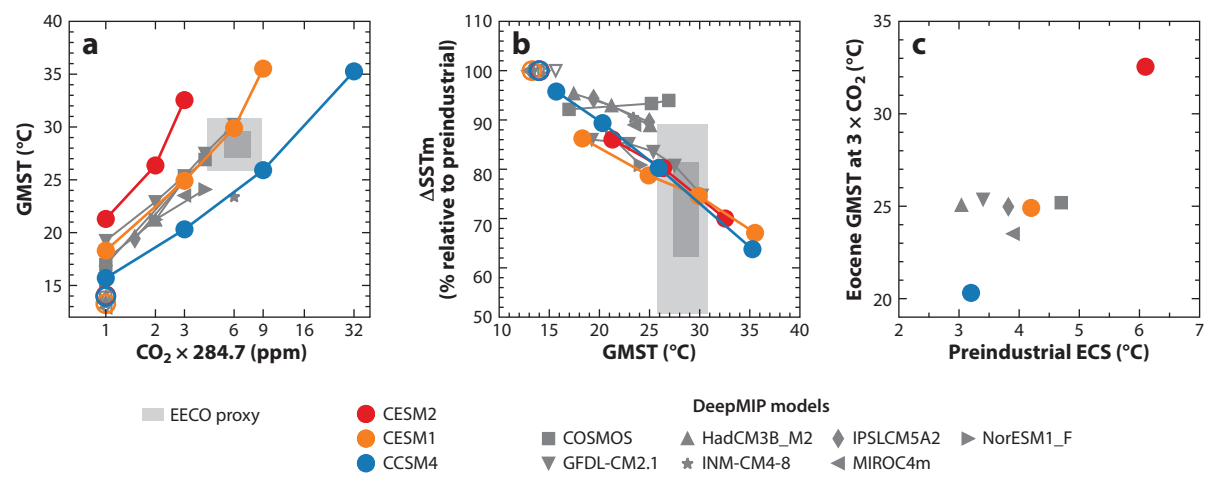


Figure 1

(a) The early Eocene GMST as a function of atmospheric CO₂ based on proxy estimates (gray boxes) and model simulations (filled markers) using CESM2 (red), CESM1 (orange), and CCSM4 (blue). The upward-pointing arrows along the top axis indicate the CO₂ level at which the model runs away with top-of-model net radiation increasing with GMST increase. Simulations from the DeepMIP are denoted by gray markers. For reference, the PI simulations are shown as open markers. The lighter/darker gray box indicates the 95% confidence interval (1 standard deviation) of proxy CO₂ and GMST. (b) The same as panel a but for the ΔSSTm in percent of the corresponding PI values. (c) Model ECS under the PI conditions against the simulated Eocene GMST with 3× PI CO₂. Note that the NorESM1_F result is from linear interpolation using two available CO₂ levels (2× and 4×). Abbreviations: ΔSSTm, meridional sea-surface temperature gradient; CCSM, Community Climate System Model; CESM, Community Earth System Model; COSMOS, COmmunity earth System ModelS; DeepMIP, Deep-Time Model Intercomparison Project; ECS, equilibrium climate sensitivity; EECO, Early Eocene Climate Optimum; GFDL, Geophysical Fluid Dynamics Laboratory; GMST, global mean surface temperature; HadCM, Hadley Centre Coupled Model; INM, Institute for Numerical Mathematics; IPSL, Institut Pierre Simon Laplace; MIROC, Model for Interdisciplinary Research on Climate; NorESM, Norwegian Earth System Model; PI, preindustrial; SST, sea-surface temperature.

We expect that exploration of the physical processes in the CESM family models will have general implications on results using the other ESMs.

We use available CESM1 simulations documented by Zhu et al. (2019) and Zhu et al. (2020a) with updates described by Tierney et al. (2022). New fully coupled CESM2 and CCSM4 simulations are performed using the same resolution (~2° atmosphere/land and ~1° ocean/sea ice) and non-CO₂ boundary conditions as the CESM1 simulations. The non-CO₂ boundary conditions follow the DeepMIP protocols and include paleogeography, vegetation, and the removal of anthropogenic aerosols and land ice sheets (Lunt et al. 2017). The new CESM2 simulations are performed with atmospheric CO₂ levels of 1, 2, and 3× the PIC level and differ from those in Zhu et al. (2020a) in the horizontal resolution (\sim 2° versus \sim 1° in the atmosphere). The new fully coupled CCSM4 simulations are performed with CO₂ levels of 1, 3, 9, and 32 × CO₂ to update the slab ocean simulations by Zhu et al. (2020a). To illustrate the importance of individual cloud and radiation processes, sensitivity simulations are performed using the CESM2 framework but with different combinations of physical parameterizations. Specifically, additional CESM2 simulations are performed with the entire CAM5 physical parameterization package, and with different versions of the cloud or radiation schemes. Some of these nondefault configurations have also been tested and validated in the simulation of the Last Glacial Maximum (LGM) (Zhu et al. 2021, 2022). For reference, we also include published Eocene simulations using the other ESMs from the DeepMIP archive (Lunt et al. 2020).

3. CURRENT STATE OF MODEL-DATA COMPARISON

3.1. Global Mean Surface Temperature and Equilibrium Climate Sensitivity

Here we present Eocene GMSTs from the three CESM versions, compare them to proxy and DeepMIP model GMSTs, and demonstrate their relationship to model ECS. Additional features emerging in the modeled Eocene GMST are also presented. Notably, all CESM simulations show an increase of ECS with global warming, and some models exhibit an apparent runaway under realistic Eocene CO₂ forcing, highlighting the need for a better understanding of these distinctive model behaviors.

3.1.1. Eocene global mean surface temperature. CESM Eocene simulations produce a wide range of GMSTs from 15.7 to 35.5°C when forced with a range of atmospheric CO₂ levels and the same non-CO₂ boundary conditions (**Figure 1***a*). Within the proxy suggested CO₂ range (~4–9×) (Anagnostou et al. 2020, see also Rae et al. 2021), CESM1 results best match the proxy with a GMST of 29.9°C at 6× PIC—warmer than the proxy median of 28.3°C but falling within the 95% CI. In contrast, CCSM4 GMSTs are too cold (23.8°C at 6× PIC interpolated using 3× and 9×)—4.5°C lower than the proxy median. CESM2 GMSTs are well above the proxy estimation and reach 32.5°C at 3× PIC. The model simulated warming in the 1× PIC simulations (relative to PI) is 7.3, 5.0, and 1.7°C in CESM2, CESM1, and CCSM4, respectively, which measures the sensitivity to non-CO₂ Eocene climate forcings including paleogeography, vegetation, and the removal of anthropogenic aerosols and land ice sheets. For comparison, the warming induced by non-CO₂ forcings in the non-CESM DeepMIP models is 3.1–3.6°C (Lunt et al. 2020). To further understand the effective radiative forcing of non-CO₂ boundary conditions and their contributions to Eocene warming, single forcing simulations need to be investigated.

The atmospheric CO_2 levels and GMSTs in the CESM series bracket the DeepMIP model results. The highest GMST simulated by a non-CESM DeepMIP model is 30.9°C in the National Oceanic and Atmospheric Administration Geophysical Fluid Dynamics Laboratory coupled model 2.1 (CM2.1) with $6 \times$ PIC, a result that is similar to CESM1. The Institute for Numerical Mathematics (INM) coupled model simulates the lowest GMST at $6 \times$ PIC, which is 23.4°C and comparable to the CCSM4 result at $6 \times$ PIC (after interpolation). The large range of GMSTs and CO_2 in the CESM series offers a unique opportunity to study the physics that determine the global warmth of the early Eocene in a consistent modeling framework.

3.1.2. Equilibrium climate sensitivity and its increase with warming. The simulated Eocene GMSTs correspond closely to the PI ECSs in the CESM series (**Figure 1***c*). At 3 × PIC, CCSM4, CESM1, and CESM2 simulate an Eocene GMST of 20.3, 24.9, and 32.5°C, respectively, which approximately scales linearly with their PI ECSs (3.2, 4.2, and 6.1°C, respectively). The close relationship between the modeled Eocene GMSTs and the PI ECSs is the physical basis for using the Eocene constraint to inform ECS in the CESM series (Zhu et al. 2020a). Interestingly, this close correspondence does not hold across DeepMIP models, i.e., the Eocene GMST is not correlated with the model ECS when the CESM series are excluded. The lack of correlation has been found in PMIP for other time periods as well (e.g., the LGM) and is likely related to the lack of high- or low-ECS models in the model ensembles, the state dependence of ECS, and the sensitivity to non-CO₂ forcing (Renoult et al. 2023). Nevertheless, Eocene simulations are effective at identifying unreasonably extreme model ECS: Both the high-ECS (such as 6.1°C in CESM2) and low-ECS (such as 1.8°C in INM) models are incompatible with Eocene proxy constraints (**Figure 1***a*). More Eocene simulations including those using the other high-ECS models will be helpful to refine the relationship between modeled Eocene GMST and the PI ECS.

All three CESMs show an increase of ECS with a background warming (shown by the increase of slope in Figure 1a). ECS increases are estimated to be 5.0 to 10.6°C in CESM2 (under a GMST range of 21.3 to 26.4°C), 4.2 to 9.6°C in CESM1 (under a GMST range of 18.3 to 29.9°C), and 2.9 to 5.1°C in CCSM4 (under a GMST range of 15.7 to 25.9°C). Given that cloud and radiation parameterizations differ substantially among the CESM series, the qualitatively consistent results seem to suggest that the increase of ECS with warming is a robust feature of warm climates. Further, the higher ECS under warmer conditions is in qualitative agreement with a recent paleoclimate data assimilation of the Paleocene-Eocene Thermal Maximum (PETM), which estimates the Eocene ECS to be 6.5°C (5.7–7.4°C; 95% CI) (Tierney et al. 2022) and much higher than the traditional IPCC range for the present-day climate (e.g., ~3°C). The increase of ECS with warming has been attributed to the increase of CO2 radiative forcing and the increase of water vapor and cloud feedbacks (Caballero & Huber 2013, Meraner et al. 2013, Zhu & Poulsen 2020, Zhu et al. 2019). While we find the increase in ECS with warming to be robust, the rate of increase is highly model dependent and needs to be better constrained from both process-based understanding and modeling and proxy data. An improved understanding can provide additional constraints on ESM simulations and is critical for constraining ECS for the present-day climate using past warm climates (Sherwood et al. 2020).

3.1.3. Model runaway. Eocene simulations run away at $4\times$ and $11\times$ PIC in CESM2 and CESM1, respectively (Figure 1a; the top-of-atmosphere net radiation increases with the increase of GMST eventually crashing the model). In contrast, the CCSM4 Eocene simulation is stable with CO₂ at 32 × PIC (and higher; not shown). We suggest that the CESM runaway reflects model deficiencies in the radiation and cloud parameterizations under extreme warm conditions (such as a GMST greater than ~35°C and a tropical SST greater than ~42°C), rather than demonstrating a physical-based runaway greenhouse due to an instability at higher temperatures and caused by the high water vapor preventing radiation to space (Ingersoll 1969). The suggestion is based on two lines or reasoning: First, there is no geological evidence for a runaway greenhouse in Earth's recent history. For example, the PETM is a stable climate in the geological record with a GMST of 34.1°C (33.1–35.5°C; 95% CI) and an atmospheric CO₂ level of ~7× PIC (1,550–2,640; 95% CI) (Tierney et al. 2022). Second, an equilibrium climate with a temperature of 57°C has been previously simulated with a limited-domain model that explicitly resolves convection and uses a more accurate line-by-line (LBL) radiation (Seeley & Wordsworth 2021). We note that other DeepMIP models also exhibit runaway simulations, albeit at different CO₂ levels [COSMOS (Community earth System ModelS) at 6x; Hadley Centre Coupled Model, version 3B (HadCM3B) at 4x; IPSL (Institut Pierre Simon Laplace) at 6×; and MIROC (Model for Interdisciplinary Research on Climate) at 4×] (Lunt et al. 2020). Diagnosing the model deficiencies under the extreme warm conditions has implications for the hothouse climate simulation, and some relevant discussion is presented in Section 4.

3.2. Spatial Distribution and Seasonal Temperatures

Here we focus on the spatial and temporal distribution of Eocene surface temperatures in model simulations. Attention is directed to the equability of Eocene temperatures—manifested as a reduced equator-to-pole temperature gradient and the notably elevated winter temperatures, characteristics consistently recognized in long-standing proxy reconstructions.

3.2.1. Meridional temperature gradient. CESM Eocene simulations show a consistent reduction of the Δ SSTm with global warming (Figure 1b). The warming induced by non-CO₂ boundary conditions decreases $\Delta SSTm$ by 5–14% in the 1× PIC simulations. The CO₂-induced warming further decreases ΔSSTm at a rate of 1.2–1.5% per °C of global warming in the CESM series, with a total reduction reaching \sim 30–36% in the warmest simulations. At the Eocene GMST range, CESM Δ SSTm falls within the range suggested by proxies. The Δ SSTm reduction in CM2.1 and NorESM1 has similar rates as in CESM; however, values in the other DeepMIP models are too small due to the insufficient sensitivity to the CO₂-induced warming (e.g., in HadCM3B and COSMOS).

The CESMs exhibit a similar rate of reduction in Δ SSTm, which can be seen in their zonal mean temperatures after linearly interpolating the simulations to the same Eocene global warming level (GMST = 28.3°C) (**Figure 2***a*). The zonal mean SSTs largely overlap with each other, with

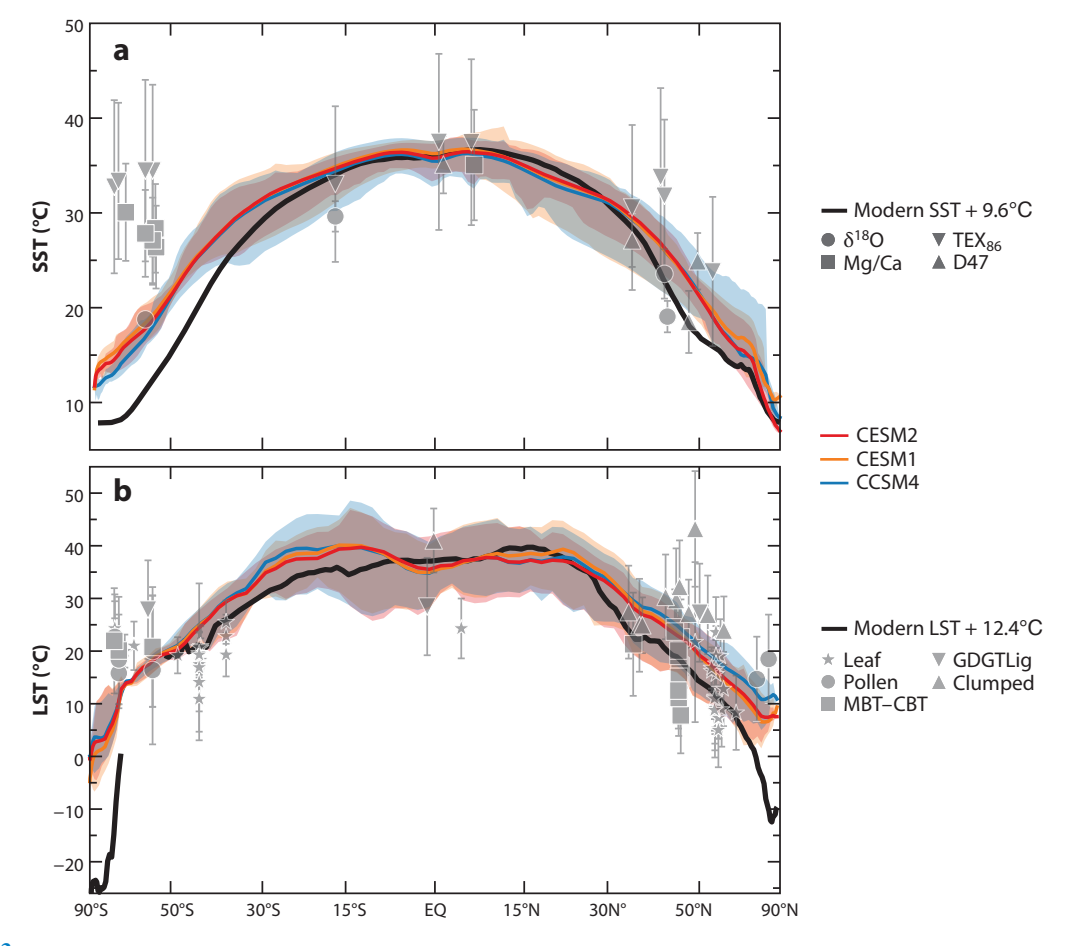


Figure 2

(a) Comparison of Eocene proxy SST reconstructions (gray markers) against zonal means in simulations (colored lines) using CESM2 (red), CESM1 (orange), and CCSM4 (blue). Error bars on proxy SSTs indicate the 95% confidence interval. Colored shading represents the full range of temperatures at the latitude in the simulation. Model results are from the linear interpolation of simulations with different CO₂ levels into the same Eocene global warmth (GMST = 28.3°C). (b) The same as panel a but for the model-data comparison of LST. Note that the x axis is sin(latitude) and thus uneven in latitudinal spacing but better illustrates the larger area of the tropics. Modern SST and LST data from the Berkeley Earth land/ocean temperature record are used for comparison (black line), which has been realigned such that they have the same tropical (15°S–15°N) means as the CESMs. Abbreviations: CCSM, Community Climate System Model; CESM, Community Earth System Model; GDGTLig, glycerol dialkyl glycerol tetraethers from lignites; GMST, global mean surface temperature; LST, land-surface temperature; MBT–CBT, methylation index of branched tetraethers and cyclization ratio of branched tetraethers; SST, sea-surface temperature.

the intermodel difference smaller than \sim 2°C over most latitudes. Similar to SSTs, the zonal mean land-surface temperatures (LSTs) also exhibit a reduction in the meridional gradient and have very small intermodel differences at the same Eocene GMST (Figure 2b). Compared to the modern zonal mean temperatures [Figure 2, which has been realigned to have the same deep tropical (15°S-15°N) temperature as the CESMs], reduction of the zonal mean temperature gradient (or equivalently, the amplification of high-latitude warming) in CESM is greater in the Southern Hemisphere than in the Northern Hemisphere. This asymmetrical warming is likely related to the preferential deep-water formation in the Southern Ocean in the simulations (Zhang et al. 2022), as well as the greater radiative forcing and elevation change from the removal of the Antarctic Ice Sheet.

The similarity of the meridional temperature structure among the CESMs is striking, given the substantial differences in their atmospheric physical parameterizations and ECSs. These results suggest that, at least in the CESM series, the polar amplification of warming (under sea ice-free conditions) is mainly due to ocean and large-scale atmosphere processes, which are similar between models, rather than details of the atmospheric physical parameterizations. These shared ocean and atmosphere processes include the coupling of the ocean-atmosphere circulation with temperature gradients, heat transport, and radiation, as well as the ocean circulation and mixing (Armour et al. 2019, Previdi et al. 2021, Russotto & Biasutti 2020, Thomas et al. 2014, Vallis 2000). Given the constancy of the meridional temperature structure between models, the results may suggest that additional forcing-feedback processes such as polar stratospheric clouds, explicitly resolved convection, aerosol-cloud interaction, and/or enhanced ocean mixing may be needed to further reduce the meridional temperature gradient (Arnold et al. 2014, Dutta et al. 2023, Korty et al. 2008, Kump & Pollard 2008, Sloan & Pollard 1998). Further exploration with non-CESMs that can simulate the proxy-inferred Eocene global warmth will be important to understand whether the meridional temperature structure in CESM is model dependent or representative of a more fundamental physical feature.

3.2.2. Regional and seasonal temperatures. Given that CESM1 at $6 \times$ PIC is one of the DeepMIP models that best matches the proxy GMST, CO₂, and ΔSSTm of the early Eocene (Figure 1) and that the CESM series exhibit similar meridional temperature structure at the same Eocene global warming level (Figure 2), we use the CESM1 6× PIC simulation (with a GMST of 29.9°C) for regional and seasonal model-data comparison.

At the regional scale, CESM1 exhibits good skill at matching individual proxy records when accounting for uncertainty in the proxy reconstruction, including the potential seasonal bias. The area-weighted root-mean-squared errors in SST and LST are 7.0 and 8.8°C, respectively, which are slightly larger than the mean uncertainty range of the records themselves (6.9°C in SST and 7.4°C in LST). The CESM1 annual mean LSTs fall within the 95% CI of 32 records (out of 81 terrestrial records) and of 71 records when accounting for potential seasonal bias in proxy (mean model temperature at any season falling into the proxy range). CESM1 annual mean SSTs fall within the range of 12 records (out of 26 marine records) and of 18 records when accounting for potential seasonal bias. In the tropics, CESM1 simulates a mean SST of ~35°C, which falls within the proxy uncertainty range of five of six tropical records (Figure 3a), with clear disagreement with the δ^{18} O record at Tanzania, which gives an Eocene SST of 29.6°C that is only \sim 2°C warmer than the modern SST. The tropical LSTs in CESM1 are ~36-40°C, which fall within the uncertainty range of the clumped isotope record in equatorial South America (41 \pm 6°C). In the Northern Hemisphere mid-latitudes, CESM1 simulates an SST and LST of ~25°C, slightly warmer than the multiple proxy average (\sim 22°C). Over the Arctic region, CESM1 simulates an LST of \sim 9°C, slightly colder than the multiple proxy average (~11°C).

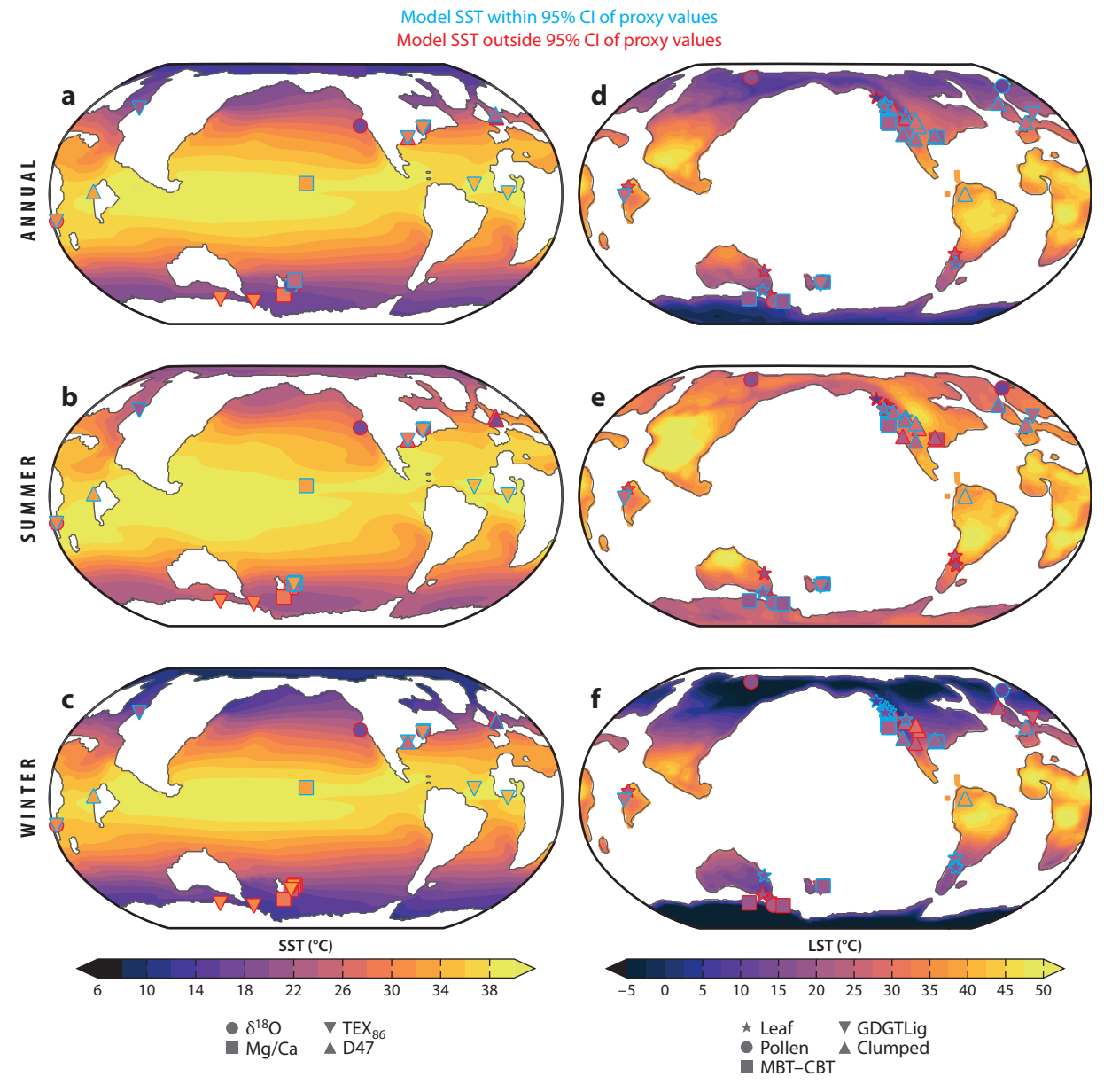


Figure 3

(a) Model simulated annual mean Eocene SST in the CESM1 6× preindustrial CO2 simulation (shading) against the proxy reconstructions (markers). The edge color of the markers is light blue if the model SST falls within the 95% confidence interval of the proxy reconstruction; otherwise, it is red. (b,c) The same as panel a but for the model-proxy comparison with the model summer (JJA in the NH and DJF in the SH) and winter (DJF in the NH and JJA in the SH) mean, respectively. (d-f) The same as panels a-c but for the model-proxy comparison of LST. Abbreviations: CESM, Community Earth System Model; DJF, December, January, February; GDGTLig, glycerol dialkyl glycerol tetraethers from lignites; JJA, June, July, August; LST, land-surface temperature; MBT-CBT, methylation index of branched tetraethers and cyclization ratio of branched tetraethers; NH, Northern Hemisphere; SH, Southern Hemisphere; SST, sea-surface temperature.

One of the largest model-data disagreements is in the southwest Pacific, around New Zealand and south of Australia, where the multi-proxy mean SSTs and LSTs are much warmer than the model results (Figure 3; see also Figure 2). Mg/Ca and TEX₈₆ records suggest very warm SSTs of \sim 31°C (average of 9 records) that are much warmer than the modeled values of \sim 20°C. Interestingly, δ¹⁸O SSTs [~28°C at Mid-Waipara River and 19°C at Hampden Beach (**Figure 2a**)] are colder than the Mg/Ca and TEX86 records, although isotope-enabled modeling using CESM1 suggests that they may be biased toward warm SSTs due to the assumptions of δ^{18} O composition of seawater that may miss the regional low values caused by the enhanced hydrological cycle (Zhu et al. 2020b). LSTs from a multi-proxy mean is ~20°C, again warmer than the model value of ~15°C. These model-data discrepancies may be due to regional- and local-scale features, such as coastal processes, that are poorly resolved in the coarse-resolution model. Higher-resolution models with better reconstructions of the finer-scale paleoclimate boundary conditions may mitigate these issues (for preliminary results from a coupled high-resolution simulation, see Section 4.2).

In the winter, CESM1 simulates a sea ice-free ocean, an above-freezing temperature over coastal land, and subfreezing temperatures in the continental interior in high latitudes. In the continental interior, winter LSTs are approximately -10°C and -5°C over high-latitude Asia and North America, respectively. Over the Antarctic, winter LSTs are approximately -10°C. Accounting for the orbital forcing that is not included in the standard 6× PIC simulation only marginally increases these temperatures by 1–3°C [not shown; orbital sensitivity runs documented in Tierney et al. (2022)]. These high-latitude subfreezing temperatures in the model seem to be incompatible with proxy indications from fossil records (e.g., the pollen record from Belkovsky Island in Russia) (Suan et al. 2017). More seasonal temperature reconstructions using a variety of proxy methods are needed to better assess the seasonal performance of ESMs and to document seasonal climate patterns, in particular the spatial extent of above-freezing temperatures (i.e., how far they extend into the interior continents). We note that the current proxy compilations focus on mean annual conditions and encourage future development of proxy compilations of seasonal conditions. Higher-resolution modeling will also be beneficial to capture the coastal ocean-atmosphere interactions and the convective low-cloud feedback that could help to maintain frost-free winters in the continental interior (Cronin & Tziperman 2015).

In summary, CESM1 provides, thus far, one of the best simulations of the early Eocene that meets the large-scale constraints in CO_2 , GMST, and Δ SSTm, as well as additional constraints from hydrological and isotope records (Cramwinckel et al. 2023, Zhu et al. 2020b).

4. TOWARD A PHYSICALLY CONSISTENT SIMULATION AND UNDERSTANDING OF HOTHOUSE CLIMATES

How can paleoclimate simulations of hothouse climates further inform ESM performance and future climate projections? Our view is that more investigations are needed to target key physical processes to ensure that their parameterizations in ESMs function realistically under hothouse conditions (i.e., ESMs produce the right answer for the right physics). In the following sections, we describe, based on recent literature and our own research with CESM, potentially fruitful avenues for improving the simulation and understanding of past warm climates.

4.1. Targeting Key Processes Using More Accurate Models

We emphasize the importance of a hierarchical modeling approach (Held 2005), taking advantage of the more accurate physics from higher-resolution and limited domain/process models. Here we highlight the radiation calculation as a fundamental part and the parameterizations of clouds and turbulence as the primary sources of uncertainty in climate modeling (e.g., Schneider et al. 2017).

4.1.1. The fundamental role of radiation. The calculation of radiation is a fundamental part of climate modeling, as it computes the transmission of radiation through the atmosphere that ultimately drives all atmospheric and oceanic motions. Radiation must be parameterized in ESMs due to the enormous computational cost to explicitly resolve the spectral radiance and transmittance over the full spectral range (see the sidebar titled Parameterization of Radiation). Similarly, as with other physical parameterizations, radiation schemes are usually developed with the presentday climate in mind and the likelihood of errors increases when parameterizations are used to make calculations outside of the range of conditions on which they are trained (e.g., Pincus et al. 2019). For example, problems have recently been identified in the radiation code, Rapid Radiative Transfer Model for General circulation model applications (RRTMG; used in CESM1 and CESM2) for idealized warm conditions (Kluft et al. 2021, Seeley & Jeevanjee 2021), due to the narrow, present-day-based temperature range of the lookup table for gas absorption. To the best of our knowledge, the role of radiation codes has not been thoroughly explored for the hothouse climates of the Eocene and the Cretaceous.

To illustrate the importance of radiation, we focus on three schemes that are available in CESM and perform (a) simple benchmarking of the clear-sky outgoing longwave radiation (OLR) against more accurate LBL calculations using idealized moist adiabatic profiles and (b) comparison of comprehensive Eocene simulations using these schemes in the CESM framework. The three radiation schemes are those used in CCSM4 [referred to as CAMRT (Community Atmosphere Model radiative transfer code) (Collins et al. 2006)], the RRTMG (Mlawer et al. 1997), and the RTE+RRTMGP [(Radiative Transfer for Energetics + Rapid Radiative Transfer Model for General circulation model applications—Parallel) (Pincus et al. 2019)]. The PyRads (Python line-by-line RADiation model) code is used for the LBL calculation (Koll & Cronin 2018).

Our simple radiation benchmarking shows that the radiation codes are not bias free and could lead to differences in forcing and feedback by more than 20% when simulating hothouse climates. The calculation uses idealized, one-dimensional moist adiabatic profiles with constant relative humidity of 80% and stratosphere temperature of 200 K (Figure 4a,b). The surface air temperature (Ts) ranges from 280 to 320 K with an increment of 1 K (Δ Ts), broadly covering the Eocene surface temperatures (Figures 2 and 3). GHGs besides CO₂ and H₂O are not considered. Two sets of longwave calculations are performed using both LBL and the three CESM radiation parameterizations: one with 1× PIC and the other with twice the value. Radiative forcing ($F_{2\times CO2}$) is calculated as \triangle OLR between 1× and 2× PIC calculations. Climate sensitivity (longwave only) is diagnosed as the forcing divided by the climate feedback parameter, which in this simple setup is $F_{2\times CO2}$ / ($\Delta OLR/\Delta Ts$). Our results show that OLR and $F_{2\times CO2}$ in the parameterized schemes differ from the LBL calculation and each other by as much as $\sim 10 \text{ Wm}^{-2}$ and 1 Wm^{-2} ($\sim 20\%$), respectively (Figures 4c,d). As a result, differences in climate sensitivity are non-negligible and large for surface temperatures above ~300 K. RRTMG results show a pronounced bias over this range and are much higher than LBL and the other schemes (Figure 4e). This bias has been reported in previous studies (Kluft et al. 2021, Seeley & Jeevanjee 2021) and remedied in the updated radiation code, RTE+RRTMPG, which uses a much wider temperature range for the lookup table (Pincus et al. 2019). We note that the above benchmarking focuses only on the clearsky broadband OLR and much work is needed to benchmark the other aspects of radiation, such as the shortwave band and the spectral distribution.

In the CESM Eocene simulations, the impact of the radiation codes on the modeled GMST could reach $\sim 5-10^{\circ}$ C (Figure 5). We perform fully coupled Eocene simulations using the same 6× CO₂ and CAM5 physical parameterizations with different radiation codes (CAMRT, RRTMG, and RTE+RRTMGP). The simulations, meant only for illustrative purposes, are integrated for 400 model years and have not reached equilibrium. At the end of 400 model years, the Eocene

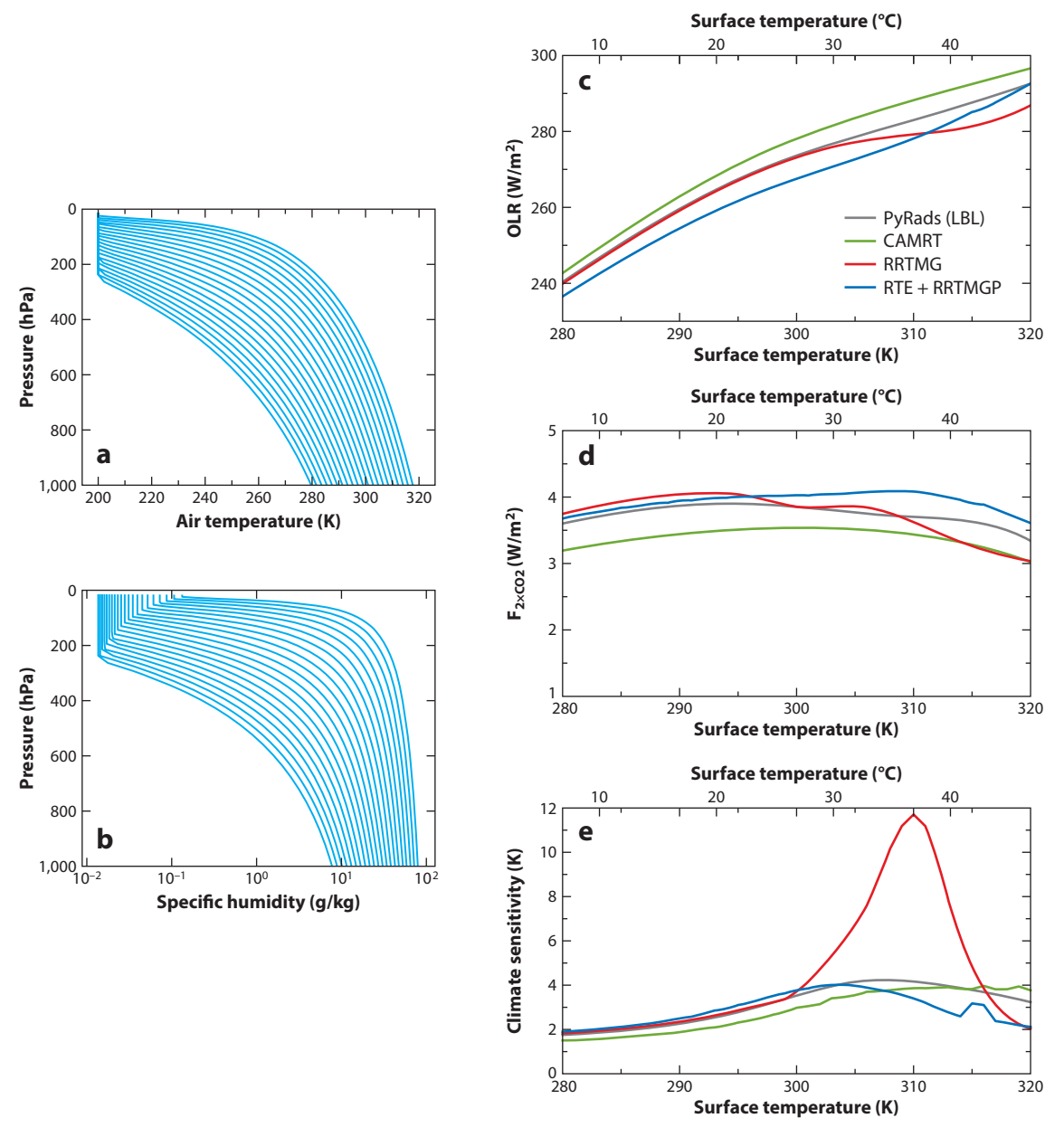
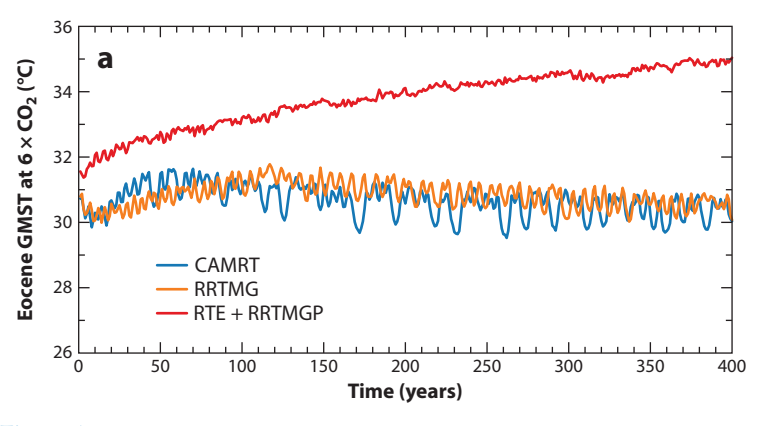


Figure 4

(a) Air temperature and (b) specific humidity of the idealized moist adiabatic profiles with a relative humidity of 80%. The profiles are generated for surface temperature from 280 to 320 K with an increment of 1 K. For illustrative purposes, every other profile is shown. (c) OLR, (d) radiative forcing from doubling CO₂ from 284.7 to 569.4 ppmw, and (e) longwave climate sensitivity, all as a function of surface temperature in Kelvin (bottom axis) and Celsius (top axis) calculated using different radiation schemes. Abbreviations: CAMRT, Community Atmosphere Model radiative transfer code; LBL, line by line; OLR, outgoing longwave radiation; PyRADS, Python line-by-line RADiation model; RRTMG, Rapid Radiative Transfer Model for General circulation model applications—Parallel.



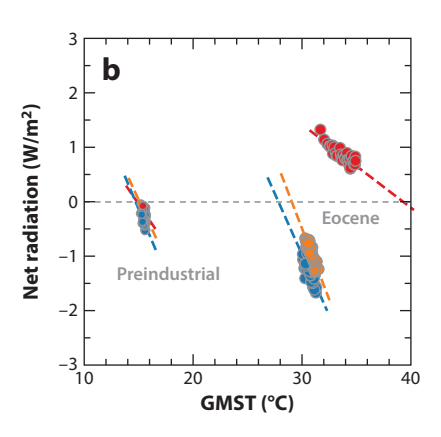


Figure 5

(a) Time series of GMST in the Eocene 6× preindustrial CO₂ simulations for different radiation schemes within CESM. (b) GMST versus the net radiation at the top of model in the Eocene and the preindustrial simulations. Shown markers are averages over each consecutive 15-year window. Dashed lines represent the linear fit between GMST and net radiation, which are used to estimate the equilibrium GMST of each simulation. Abbreviations: CAMRT, Community Atmosphere Model radiative transfer code; CESM, Community Earth System Model; GMST, global mean surface temperature; RRTMG, Rapid Radiative Transfer Model for General circulation model applications; RTE+RRTMGP, Radiative Transfer for Energetics + Rapid Radiative Transfer Model for General circulation model applications—Parallel.

GMSTs differ by ~5°C and are projected to potentially increase to 10°C in the equilibrium state (estimation using linear extrapolation between the top-of-atmosphere net radiation and GMST) (Figure 5b). In contrast to the Eocene, PI simulations share similar GMST and top-of-atmosphere net radiation, highlighting the importance of benchmarking radiation codes using conditions outside the present-day climate. Interestingly, GMST differences between the RRTMG and CAMRT simulations are relatively small and projected to be ~2°C, suggesting an overall small impact from the longwave bias in RRTMG (Figure 4), likely due to compensating errors in the system or masking of the bias by other processes. The estimated impact on GMST from different radiation schemes (2–10°C) is comparable in magnitude to the contribution from uncertainties in the Eocene boundary condition and other aspects of the model physics (e.g., Figure 1a). These results emphasize the importance of radiation parameterizations and suggest that radiation codes should be benchmarked and investigated more frequently for paleoclimate with much higher or lower GHGs and temperatures to improve their fidelity.

4.1.2. Clouds and turbulence. The significance of clouds and turbulence for the simulation of hothouse climates has been emphasized in recent modeling studies with varying complexity and spatial scope (Sagoo et al. 2013, Schneider et al. 2019, Seeley & Wordsworth 2021, Zhu et al. 2019). The importance of clouds and turbulence underscores that paleoclimate data of past hothouse climates can be used to assess the related parameterizations in ESMs because a physically consistent simulation of hothouse climate should accurately represent these processes.

Here we use perturbed physics simulations in CESM2 to demonstrate the importance of cloud parameterizations for hothouse climates and to highlight the potential for employing past climates to assess key cloud parameterizations. We test the relative importance of different cloud parameterizations (see the sidebars titled Parameterization of Boundary-Layer Moist Turbulence and Clouds and Parameterization of Cloud Microphysics and Ice Nucleation) in coupled Eocene simulations by switching (one at a time) key cloud schemes in CESM2 to the older CESM1 scheme. We investigate three cloud schemes including cloud microphysics, ice nucleation, and

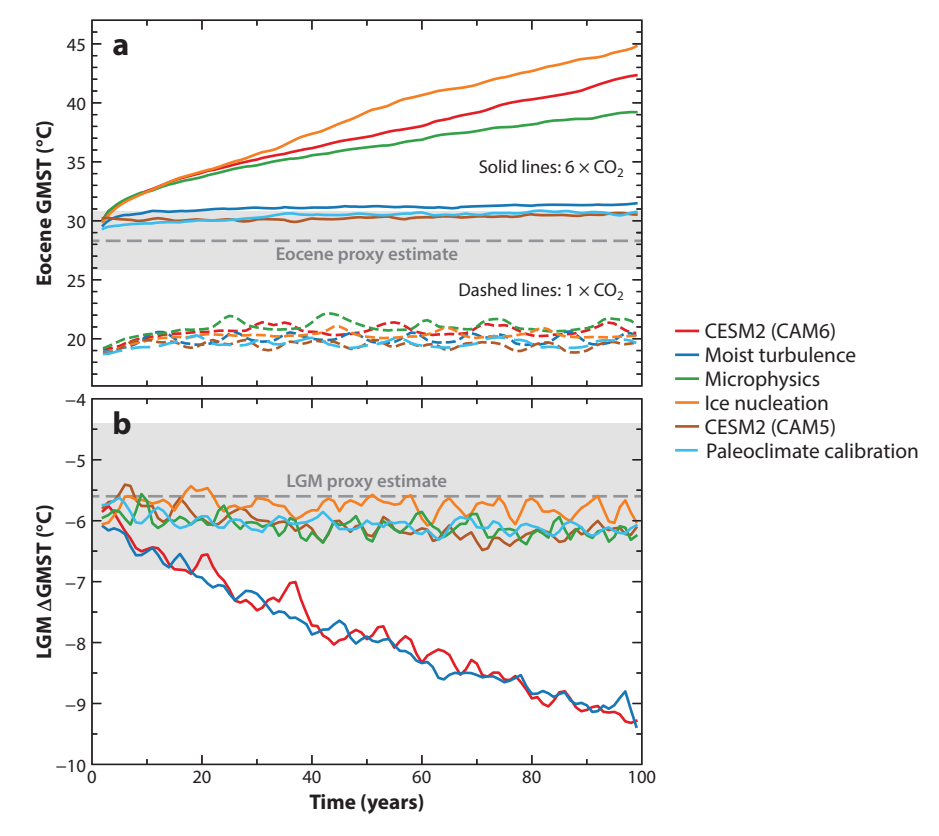


Figure 6

(a) GMST in the Eocene simulations with 6× PIC (solid colored lines) and 1× PIC (dashed colored lines) and the comparison with proxy-based estimation (black dashed line) and the 95% confidence interval (gray patch). Shown are time series from simulations done with the standard CESM2 (CAM6) (red) and CESM2 (CAM5) (brown) and the CESM2 (CAM6)-based sensitivity simulations with cloud scheme switched to the CAM5 version one at a time: the moist turbulence (blue), microphysics (green), and ice nucleation (orange) schemes. A paleoclimate-calibrated configuration based on CESM2 (CAM6) that matches the temperature of both the early Eocene and the LGM is also shown (cyan). Paleoclimate calibration includes fixes in the cloud microphysics (Zhu et al. 2022) and new tuning of the moist turbulence scheme to enhance the damping of the asymmetrical mixing. (b) The same as panel a but for the sensitivity simulations on the LGM [shown are the GMST differences between the LGM and PI simulations (see Zhu et al. 2022)]. Plotted are three-year running means. All simulations are initialized from the quasi-equilibrium simulations using CESM1.2 with the same boundary conditions. Abbreviations: CAM, Community Atmosphere Model; CESM, Community Earth System Model; GMST, global mean surface temperature; LGM, Last Glacial Maximum; PI, preindustrial; PIC, preindustrial CO₂.

moist turbulence, all of which differ substantially between the CESM versions and have been found to greatly impact CESM2's ECS and LGM simulation (Gettelman et al. 2019, Zhu et al. 2022). The CESM2 Eocene simulation runs away at 6× PIC with GMST increasing linearly to more than 42°C after 100 model years (Figure 6a). In contrast, when we switch all three atmospheric physical parameterizations to the CESM1 versions, the simulation is stable with a GMST of ~30°C and comparable to the CESM1 simulation by Zhu et al. (2019) (and is in overall good agreement with Eocene reconstructions). The moist turbulence scheme contributes the most to the difference between models, and the version in CESM1 leads to a stabilization of GMST at \sim 31°C. The 1× PIC simulations are much less sensitive to choices of cloud schemes

with differences in GMSTs less than 2°C, again highlighting the value of investigating model behavior over a wide range of climate conditions. These results suggest that hothouse climates such as the early Eocene strongly depend on the boundary-layer turbulence and convection processes (Schneider et al. 2019, Seeley & Wordsworth 2021) and thus can provide assessment of the parameterizations of these processes in ESMs.

The assessment of model parameterizations using both Eocene and LGM constraints presents an interesting contrast (**Figure 6b**); together, they illustrate the potential and necessity of using both hothouse and icehouse climates to inform and improve cloud parameterizations. In contrast to the Eocene, the LGM simulation is not sensitive to the moist turbulence scheme but rather to the microphysics and ice nucleation schemes (Zhu et al. 2022). The weaker influence of the microphysics and ice nucleation schemes on hothouse climates is consistent with a substantially smaller proportion of mixed-phase clouds (i.e., clouds containing water vapor, ice particles, and coexisting supercooled liquid droplets) under extreme warm conditions (Zhu & Poulsen 2020).

Further exploration with CESM2 shows that a paleoclimate-calibrated configuration of the model can be developed that meets both temperature constraints of the early Eocene and the LGM (**Figure 6**). The paleo-calibrated version includes fixes in cloud microphysics (Zhu et al. 2022) and new parameter tuning to increase the Newtonian damping of the asymmetrical mixing in the moist turbulence scheme. The stronger damping weakens the boundary-layer turbulence and is hypothesized to reduce and delay the disappearance of low clouds as temperature increases and thus stabilize the Eocene simulation. With these modifications, CESM2 matches the paleoclimate constraints and simulates an ECS of 3.0°C, which is consistent with recent assessment reports (IPCC 2021, Sherwood et al. 2020).

4.2. Taking Advantage of High-Resolution Earth System Models

One recent development in the climate modeling community is the possibility of running coupled ESMs at much higher horizontal resolution. A recent international effort developed a version of CESM1 for high-resolution applications (CESM1-HR) and performed coupled simulations of the present and future climates with a horizontal resolution of ~0.25° in the atmosphere and land and ~0.1° in the ocean and sea ice, which are an order of magnitude finer than the traditional low resolutions (Chang et al. 2020). At this finer resolution, CESM1-HR better resolves ocean eddies (see the sidebar titled Ocean Eddies) and topography/bathymetry and simulates much more realistic coastal upwelling systems, tropical cyclones, atmospheric rivers, and other hydrological processes (Chang et al. 2020).

Here we present preliminary results from an Eocene simulation with 3× PIC using CESM1-HR. **Figure 7***a* shows a snapshot of the daily SST, which features finer structures, including ocean eddies, a sharper temperature contrast along ocean fronts and in coastal regions, and SST cold

OCEAN EDDIES

Ocean mesoscale eddies (the so-called weather systems of the ocean) determine many processes in the oceans, such as heat and nutrient transport, especially in marginal ocean areas with more complex geographies and bathymetry. A horizontal ocean grid size of ~ 10 km is needed to resolve the mesoscale eddies. Consequently, mesoscale eddies must be parameterized in global ocean models with grid sizes of ~ 100 km. Some of the newer ESMs, such as CESM1-HR (the Community Earth System Model for high-resolution applications with a horizontal grid of $\sim 0.1^{\circ}$), explicitly resolve the mesoscale eddies and are considered to provide a better representation of these systems, allowing reassessment of how ocean currents change with global warming and how this will affect, for example, regional and global temperatures, hydrological cycle, surface water ecosystems, carbon cycling, or coastal ice shelves.

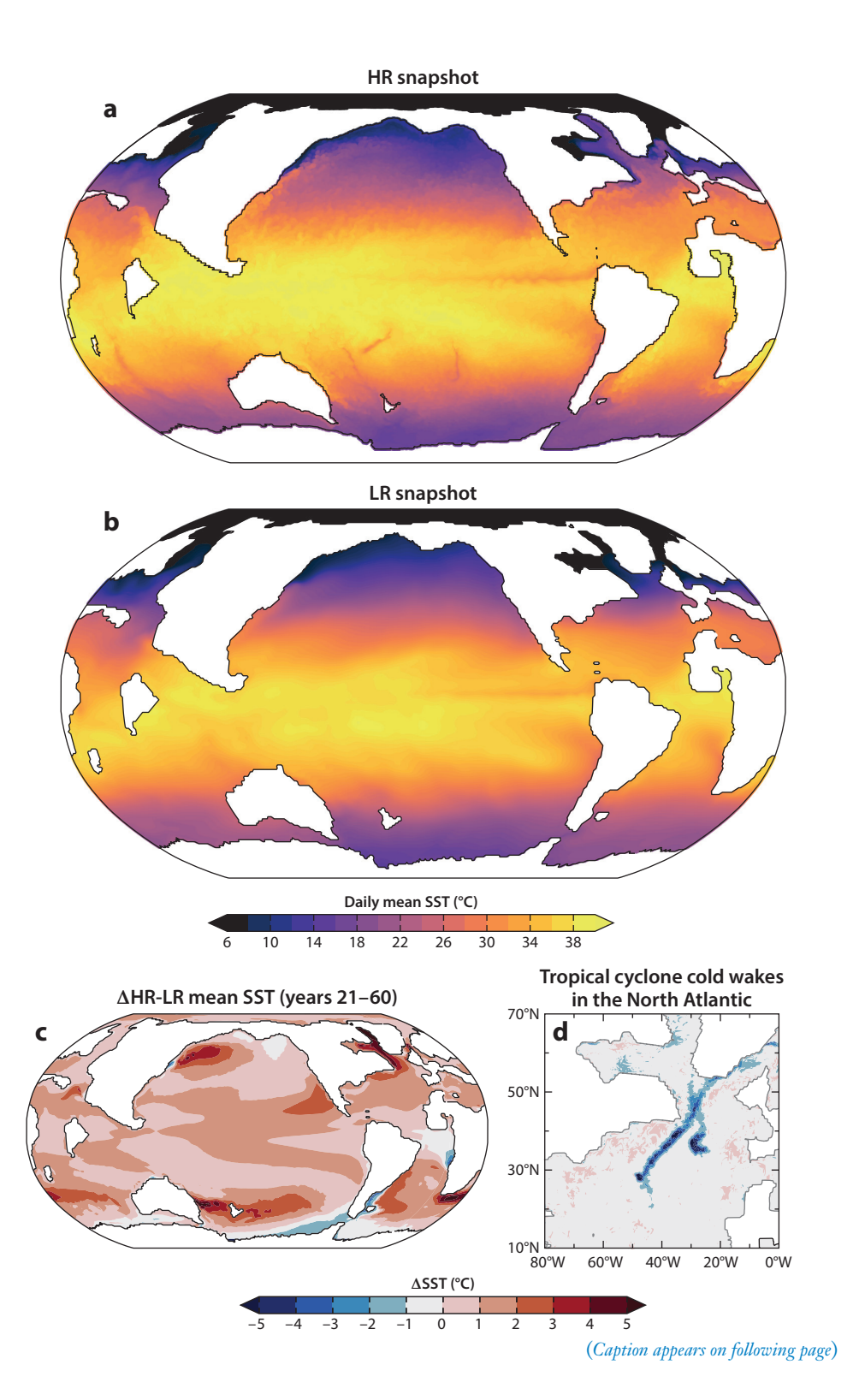


Figure 7 (Figure appears on preceding page)

(a) A snapshot of daily mean SST in the HR Eocene simulation using CESM_x-HR with $3 \times$ preindustrial CO₂. Note the fine-scale features, such as those associated with ocean eddies, fronts, and coastal circulations. (b) The same as panel a but for an SST snapshot from the LR simulation. The HR simulation was initialized from ocean states interpolated from the LR simulation. (c) Differences in the multi-decade mean SST (averaged between year 21 and 60) between HR and LR simulations. (d) SST cold wakes underneath two tropical cyclones over the North Atlantic in the HR simulation, calculated as minimum daily SST minus the mean during the tropical cyclone events. SST snapshots in panels a and b and the cold wakes in panel d are randomly chosen to illustrate the unique benefits of the HR simulation. Abbreviations: CESM, Community Earth System Model; HR, high resolution; LR, low resolution; SST, sea-surface temperature.

wakes associated with tropical cyclones, when compared to the low-resolution SST in **Figure 7***b*. The explicit resolution of ocean eddies and fine-scale coastal processes and air-sea interactions impact the SST climatology at longer timescales. **Figure 7***c* shows the differences in the 40-year mean SST between the high- and low-resolution simulations. The high-resolution simulation exhibits warmer SSTs over the mid-latitudes and subtropics, which may lead to warmer global temperatures and a weaker meridional temperature gradient. The changes caused by simulation of ocean eddies, fronts, and coastal winds are likely amplified by climate feedbacks (e.g., the cloud feedback). It will be interesting to see how these differences manifest at centennial timescales after the simulation has been carried out longer. Nevertheless, results here seem to suggest that high-resolution paleoclimate simulations are likely to produce significantly different global and regional temperatures from their low-resolution counterparts.

Figure 7*d* shows a zoom in on SST anomalies underneath two tropical cyclones over the North Atlantic Ocean. The SST anomalies are calculated using the minimum daily SST minus the mean values centered around these events. The cold wakes—waters left behind following the cyclone passage—are in excess of 5°C cooler and associated with enhanced upper ocean mixing and downward heat pumping. It has been long hypothesized that tropical cyclones stir the upper ocean, increase the meridional heat transport, and contribute to a reduced meridional temperature gradient in past hothouse climates (Emanuel 2002, Korty et al. 2008, Sriver & Huber 2007). Coupled high-resolution simulations will allow testing of this hypothesis, for the first time, in a physically consistent framework.

We suggest that emerging coupled high-resolution simulations should be employed more frequently to test hypotheses regarding the climate dynamics of hothouse climates and to study the weather and climate extremes and the hydrological cycle under warm conditions. Better resolved coastal processes are also critical for improving model-data comparisons for past climates, as most proxy records are from coastal or shelf environments. To fully take advantage of high-resolution capabilities, paleoclimate boundary conditions (especially paleogeography and paleobathymetry) also need to be improved and ideally resolved at the scale of the model.

4.3. Leveraging the Increasing Complexity of Earth System Models

In parallel with improvements in the resolution of ESMs, the complexity and realism of ESMs has been continually growing. The increased complexity allows research to test hypotheses in a consistent Earth system framework. To name a few, the stratospheric dynamics and chemistry could be explored using the state-of-the-art climate-chemistry models, for example to test the hypothesis that polar stratospheric clouds contribute to the warmth of polar winters. The role of biogenic aerosols and their interaction with clouds could be investigated using ESMs with prognostic aerosol emissions from vegetation and ocean biology. Vegetation and the two-way interaction with hydroclimate could be studied using the dynamic vegetation capability of ESMs and the paleoclimate vegetation reconstruction. The model-data comparison could be improved

when using the new geochemical tracers in ESMs (such as water and carbon isotopes, neodymium isotopes) (Brady et al. 2019, Gu et al. 2019, Zhu et al. 2020b). To further explore the Earth system feedback, a combined modeling approach could provide further insights, such as an offline coupling of complex ESMs and carbon cycle-enabled models with intermediate complexity (Penn et al. 2018).

5. CONCLUSIONS

Significant progress has been achieved in the modeling and understanding of past hothouse climates over the last 40 years to the point where some ESMs can now credibly simulate the large-scale features of these hothouse worlds. This progress has been the result of both improvements in the models—including their capabilities, complexity, spatial resolution, and boundary conditions—and improvements in the quality, number, and interpretation of proxy climate data. Over the last 40 years, modeling past hothouse climates has evolved from a novelty to be a critical validation of ESM performance. While past hothouse climates will never be a perfect analogue for our future climate, they provide the only opportunities to evaluate the capabilities of models under the CO₂ levels of the future.

Below we offer a summary of the current state of the simulation of past hothouse climates and future directions for advancing the field:

SUMMARY POINTS

- 1. Past warm climates represent the only real-world data points on how the Earth system responds to CO₂ levels in excess of those experienced during the historical time period. These warm periods offer unique opportunities to assess the performance of Earth system models (ESMs) and ultimately to improve our understanding and projection of the future climate.
- 2. ESMs [such as the Community Earth System Model version 1 (CESM1)] are now able to simulate the large-scale features of hothouse climates of the early Eocene. In CESM, the simulated global mean surface temperature (GMST) is very sensitive to atmospheric parameterizations of radiation and clouds. The equator-to-pole temperature gradient, however, is largely insensitive to CESM versions when model results are interpolated into the same level of GMST. This result indicates that the strength of polar amplified warming (under a sea ice-free condition) could depend more on the oceanic and largescale atmospheric processes rather than directly on the atmospheric parameterizations.
- 3. Model-data discrepancies in Eocene surface temperatures remain at regional and seasonal scales. In particular, the proxy temperatures over the Southern Ocean (specifically, the southwest Pacific, around New Zealand and south of Australia), as well as the warm continental winter temperatures and the reduced seasonality, are still challenging to simulate using ESMs.

FUTURE ISSUES

1. Our and others' work has shown that the ability to simulate past warm climates is critically dependent on the model physics (i.e., the parameterizations) and that hothouse climates can be used to assess the performance of the model physics under high CO₂ levels. The paleoclimate modeling community has an opportunity to further close the gap in the understanding and assessment of physical processes by taking a hierarchical modeling approach that leverages the accuracy of models with a limited scope in physics and region.

- 2. Emerging improvements in spatial resolution and model complexity offer opportunities to address long-standing questions about the processes that influence fundamental climate features, for example the equator-to-pole gradient. We encourage early adoption of these improvements by the paleoclimate modeling community to both advance our understanding of past climates and provide assessment and fuller perspective of their influences across climate states.
- 3. Further improvements in the spatial coverage of proxy temperatures of past hothouse climates are needed to reduce the uncertainty in estimating both the GMST and the equator-to-pole gradient. In particular, the current estimation of Eocene equator-topole temperature gradient relies on 6 tropical sea-surface temperature (SST) records (many of which are from coastal or upwelling regions and may not represent the tropics well) and the use of deep ocean temperature as a substitute for the polar SSTs due partly to the lack of data coverage.
- 4. The evolution of the tropical SST reconstruction over the past few decades demonstrates the value of a multi-proxy approach and the need for adequate consideration of uncertainties from proxy calibration and other sources. We encourage the proxy data community to continue to use a multi-proxy approach and to explore proxy uncertainties to better reconstruct both mean temperature and its variability from seasonal to orbital timescales.
- 5. Finally, the simulations of past climates are only as good as the boundary conditions that define them. Refinement of atmospheric CO2 estimates and additional constraints on other non-CO₂ paleoclimate boundary conditions, especially paleogeography, paleotopography, and vegetation, are needed, so that the past hothouse climates can provide tighter constraints on important processes in ESM simulations.

DISCLOSURE STATEMENT

The authors are not aware of any affiliations, memberships, funding, or financial holdings that might be perceived as affecting the objectivity of this review.

ACKNOWLEDGMENTS

This work was supported by National Science Foundation (NSF) grant 2202777 to J.Z. and NSF grant 2309580 and Heising-Simons Foundation grant 2016-015 to C.J.P. The CESM project is supported primarily by the NSF. This material is based upon work supported by the National Center for Atmospheric Research (NCAR), which is a major facility sponsored by the NSF under Cooperative Agreement 1852977. Computing and data storage resources, including the Cheyenne (doi:10.5065/D6RX99HX) and Derecho (doi:10.5065/qx9a-pg09) supercomputers, were provided by the Computational and Information Systems Laboratory at NCAR. We thank Jim Edwards for porting the high-resolution CESM to the supercomputer Derecho. We thank Brian Medeiros and others for incorporating the RTE+RRTMGP radiation code into

CESM. We acknowledge the NCAR Accelerated Scientific Discovery computer allocation for extensive use of Derecho at the NCAR-Wyoming supercomputer center.

LITERATURE CITED

- Abbot DS, Tziperman E. 2008. Sea ice, high-latitude convection, and equable climates. Geophys. Res. Lett. 35:L03702
- Anagnostou E, John EH, Babila TL, Sexton PF, Ridgwell A, et al. 2020. Proxy evidence for state-dependence of climate sensitivity in the Eocene greenhouse. Nat. Commun. 11:4436
- Armour KC, Siler N, Donohoe A, Roe GH. 2019. Meridional atmospheric heat transport constrained by energetics and mediated by large-scale diffusion. *J. Clim.* 32(12):3655–80
- Arnold NP, Branson M, Burt MA, Abbot DS, Kuang Z, et al. 2014. Effects of explicit atmospheric convection at high CO₂. PNAS 111:10943-48
- Barron EJ. 1983. A warm, equable Cretaceous: the nature of the problem. Earth-Sci. Rev. 19:305-38
- Barron EJ. 1987. Eocene equator-to-pole surface ocean temperatures: a significant climate problem? Paleoceanography 2:729-39
- Barron EJ, Washington WM. 1984. The role of geographic variables in explaining paleoclimates: results from Cretaceous climate model sensitivity studies. J. Geophys. Res. 89(D1):1267-79
- Barron EJ, Washington WM. 1985. Warm Cretaceous climates: high atmospheric CO₂ as a plausible mechanism. In The Carbon Cycle and Atmospheric CO2: Natural Variations Archean to Present, ed. ET Sundquist, WS Broecker, pp. 546–53. Washington, DC: Am. Geophys. Union
- Beerling DJ, Fox A, Stevenson DS, Valdes PJ. 2011. Enhanced chemistry-climate feedbacks in past greenhouse worlds. PNAS 108:9770-75
- Bernard S, Daval D, Ackerer P, Pont S, Meibom A. 2017. Burial-induced oxygen-isotope re-equilibration of fossil foraminifera explains ocean paleotemperature paradoxes. Nat. Commun. 8:1134
- Bice KL, Birgel D, Meyers PA, Dahl KA, Hinrichs KU, Norris RD. 2006. A multiple proxy and model study of Cretaceous upper ocean temperatures and atmospheric CO₂ concentrations. Paleoceanography 21:PA2002
- Brady E, Stevenson S, Bailey D, Liu Z, Noone D, et al. 2019. The connected isotopic water cycle in the Community Earth System Model version 1. J. Adv. Model. Earth Syst. 11:2547-66
- Bush ABG, Philander SGH. 1997. The late Cretaceous: simulation with a coupled atmosphere-ocean general circulation model. Paleoceanography 12:495-516
- Caballero R, Huber M. 2013. State-dependent climate sensitivity in past warm climates and its implications for future climate projections. PNAS 110:14162-67
- Chang P, Zhang S, Danabasoglu G, Yeager SG, Fu H, et al. 2020. An unprecedented set of high-resolution earth system simulations for understanding multiscale interactions in climate variability and change. 7. Adv. Model. Earth Syst. 12:e2020MS002298
- Collins WD, Bitz CM, Blackmon ML, Bonan GB, Bretherton CS, et al. 2006. The Community Climate System Model version 3 (CCSM3). J. Clim. 19:2122-43
- Covey C, Barron E. 1988. The role of ocean heat transport in climatic change. Sci. Rev. 24:429-45
- Cramer BS, Miller KG, Barrett PJ, Wright JD. 2011. Late Cretaceous-Neogene trends in deep ocean temperature and continental ice volume: reconciling records of benthic foraminiferal geochemistry (δ^{18} O and Mg/Ca) with sea level history. J. Geophys. Res. 116(C12):C12023
- Cramwinckel MJ, Burls NJ, Fahad AA, Knapp S, West CK, et al. 2023. Global and zonal-mean hydrological response to Early Eocene warmth. Paleoceanogr. Paleoclimatol. 38:e2022PA004542
- Cronin TW, Tziperman E. 2015. Low clouds suppress Arctic air formation and amplify high-latitude continental winter warming. PNAS 112:11490-95
- Danabasoglu G, Lamarque J-F, Bacmeister J, Bailey DA, DuVivier AK, et al. 2020. The Community Earth System Model version 2 (CESM2). J. Adv. Model. Earth Syst. 12:e2019MS001916
- Dutta D, Jucker M, Sherwood SC, Meissner KJ, Sen Gupta A, Zhu J. 2023. Early Eocene low orography and high methane enhance Arctic warming via polar stratospheric clouds. Nat. Geosci. 16(11):1027–32
- Emanuel K. 2002. A simple model of multiple climate regimes. 7. Geophys. Res. 107(D9):ACL 4-1-ACL 4-10 Evans D, Sagoo N, Renema W, Cotton LJ, Müller W, Todd JA. 2018. Eocene greenhouse climate revealed

by coupled clumped isotope-Mg/Ca thermometry. PNAS 115:1174–79

- Farrell BF. 1990. Equable climate dynamics. J. Atmos. Sci. 47:2986-95
- Foster GL, Royer DL, Lunt DJ. 2017. Future climate forcing potentially without precedent in the last 420 million years. *Nat. Commun.* 8:14845
- Gent PR, Danabasoglu G, Donner LJ, Holland MM, Hunke EC, et al. 2011. The Community Climate System Model version 4. 7. Clim. 24:4973–91
- Gettelman A, Hannay C, Bacmeister JT, Neale RB, Pendergrass AG, et al. 2019. High climate sensitivity in the Community Earth System Model version 2 (CESM2). *Geophys. Res. Lett.* 46:8329–37
- Gettelman A, Kay JE, Shell KM. 2012. The evolution of climate sensitivity and climate feedbacks in the community atmosphere model. *J. Clim.* 25:1453–69
- Green JAM, Huber M. 2013. Tidal dissipation in the early Eocene and implications for ocean mixing. Geophys. Res. Lett. 40:2707–13
- Greenwood DR, Wing SL. 1995. Eocene continental climates and latitudinal temperature gradients. *Geology* 23:1044–48
- Gu S, Liu Z, Jahn A, Rempfer J, Zhang J, Joos F. 2019. Modeling neodymium isotopes in the ocean component of the Community Earth System Model (CESM1). 7. Adv. Model. Earth Syst. 11:624–40
- Held IM. 2005. The gap between simulation and understanding in climate modeling. *Bull. Am. Meteorol. Soc.* 86:1609–14
- Hewitt H, Fox-Kemper B, Pearson B, Roberts M, Klocke D. 2022. The small scales of the ocean may hold the key to surprises. *Nat. Clim. Change* 12:496–99
- Ho SL, Laepple T. 2016. Flat meridional temperature gradient in the early Eocene in the subsurface rather than surface ocean. *Nat. Geosci.* 9:606–10
- Hollis CJ, Dunkley Jones T, Anagnostou E, Bijl PK, Cramwinckel MJ, et al. 2019. The DeepMIP contribution to PMIP4: methodologies for selection, compilation and analysis of latest Paleocene and early Eocene climate proxy data, incorporating version 0.1 of the DeepMIP database. Geosci. Model Dev. 12:3149–206
- Hollis CJ, Taylor KWR, Handley L, Pancost RD, Huber M, et al. 2012. Early Paleogene temperature history of the Southwest Pacific Ocean: reconciling proxies and models. *Earth Planet. Sci. Lett.* 349–350:53–66
- Huber BT, MacLeod KG, Watkins DK, Coffin MF. 2018. The rise and fall of the Cretaceous Hot Greenhouse climate. *Global Planet. Change* 167:1–23
- Huber M. 2008. A hotter greenhouse? Science 321:353-54
- Huber M, Caballero R. 2011. The early Eocene equable climate problem revisited. Clim. Past 7:603-33
- Huber M, Sloan LC. 2001. Heat transport, deep waters, and thermal gradients: coupled simulation of an Eocene greenhouse climate. *Geophys. Res. Lett.* 28:3481–84
- Hurrell JW, Holland MM, Gent PR, Ghan S, Kay JE, et al. 2013. The Community Earth System Model: a framework for collaborative research. *Bull. Am. Meteorol. Soc.* 94:1339–60
- Ingersoll AP. 1969. The runaway greenhouse: a history of water on Venus. 7. Atmos. Sci. 26:1191-98
- Inglis GN, Bragg F, Burls NJ, Cramwinckel MJ, Evans D, et al. 2020. Global mean surface temperature and climate sensitivity of the early Eocene Climatic Optimum (EECO), Paleocene–Eocene Thermal Maximum (PETM), and latest Paleocene. *Clim. Past* 16:1953–68
- Inglis GN, Farnsworth A, Lunt D, Foster GL, Hollis CJ, et al. 2015. Descent toward the Icehouse: Eocene sea surface cooling inferred from GDGT distributions. *Paleoceanography* 30:1000–20
- IPCC (Intergov. Panel Clim. Change). 2021. Climate Change 2021: The Physical Science Basis. Contribution of Working Group I to the Sixth Assessment Report of the Intergovernmental Panel on Climate Change, ed. V Masson-Delmotte, P Zhai, A Pirani, SL Connors, C Péan, et al. Cambridge, UK: Cambridge Univ. Press
- Kay JE, Hillman BR, Klein SA, Zhang Y, Medeiros B, et al. 2012. Exposing global cloud biases in the Community Atmosphere Model (CAM) using satellite observations and their corresponding instrument simulators. J. Clim. 25:5190–207
- Kiehl JT, Shields CA. 2013. Sensitivity of the Palaeocene–Eocene Thermal Maximum climate to cloud properties. *Philos. Trans. R. Soc. A* 371:20130093
- Kirk-Davidoff DB, Schrag DP, Anderson JG. 2002. On the feedback of stratospheric clouds on polar climate. Geophys. Res. Lett. 29:51-1-51-4
- Kluft L, Dacie S, Brath M, Buehler SA, Stevens B. 2021. Temperature-dependence of the clear-sky feedback in radiative-convective equilibrium. *Geophys. Res. Lett.* 48:e2021GL094649

- Koll DDB, Cronin TW. 2018. Earth's outgoing longwave radiation linear due to H2O greenhouse effect.
- Korasidis VA, Wing SL, Shields CA, Kiehl JT. 2022. Global changes in terrestrial vegetation and continental climate during the Paleocene-Eocene Thermal Maximum. Paleoceanogr: Paleoclimatol. 37(4):e2021PA004325
- Korty RL, Emanuel KA, Scott JR. 2008. Tropical cyclone-induced upper-ocean mixing and climate: application to equable climates. J. Clim. 21:638–54
- Kump LR, Pollard D. 2008. Amplification of Cretaceous warmth by biological cloud feedbacks. Science 320:195 Lunt DJ, Bragg F, Chan WL, Hutchinson DK, Ladant JB, et al. 2020. DeepMIP: model intercomparison of early Eocene climatic optimum (EECO) large-scale climate features and comparison with proxy data. Clim. Past Discuss. 2020:1-27
- Lunt DJ, Dunkley Jones T, Heinemann M, Huber M, LeGrande AN, et al. 2012. A model-data comparison for a multi-model ensemble of early Eocene atmosphere-ocean simulations: EoMIP. Clim. Past 8:1717-36
- Lunt DJ, Huber M, Anagnostou E, Baatsen MLJ, Caballero R, et al. 2017. The DeepMIP contribution to PMIP4: experimental design for model simulations of the EECO, PETM, and pre-PETM (version 1.0). Geosci, Model Dev. 10:889-901
- Meckler AN, Sexton PF, Piasecki AM, Leutert TJ, Marquardt J, et al. 2022. Cenozoic evolution of deep ocean temperature from clumped isotope thermometry. Science 377:86-90
- Meraner K, Mauritsen T, Voigt A. 2013. Robust increase in equilibrium climate sensitivity under global warming. Geophys. Res. Lett. 40:5944-48
- Mlawer EJ, Taubman SJ, Brown PD, Iacono MJ, Clough SA. 1997. Radiative transfer for inhomogeneous atmospheres: RRTM, a validated correlated-k model for the longwave. 7. Geophys. Res. 102(D14):16663-
- Morrison H, van Lier-Walqui M, Fridlind AM, Grabowski WW, Harrington JY, et al. 2020. Confronting the challenge of modeling cloud and precipitation microphysics. J. Adv. Model. Earth Syst. 12:e2019MS001689
- Nooteboom PD, Baatsen M, Bijl PK, Kliphuis MA, van Sebille E, et al. 2022. Improved model-data agreement with strongly eddying ocean simulations in the middle-late Eocene. Paleoceanogr. Paleoclimatol. 37:e2021PA004405
- Norris R, Corfield R, Hayes-Baker K, Huber B, MacLeod K, Wing S. 1999. Mountains and Eocene climate. In Warm Climates in Earth History, ed. B Huber, K MacLeod, S Wing, pp. 161-96. Cambridge, UK: Cambridge Univ. Press
- O'Brien CL, Robinson SA, Pancost RD, Sinninghe Damsté JS, Schouten S, et al. 2017. Cretaceous sea-surface temperature evolution: constraints from TEX₈₆ and planktonic foraminiferal oxygen isotopes. Sci. Rev.
- O'Connor LK, Robinson SA, Naafs BDA, Jenkyns HC, Henson S, et al. 2019. Late Cretaceous temperature evolution of the southern high latitudes: a TEX₈₆ perspective. Paleoceanogr. Paleoclimatol. 34:436–54
- Otto-Bliesner BL, Brady EC, Shields C. 2002. Late Cretaceous ocean: coupled simulations with the National Center for Atmospheric Research climate system model. J. Geophys. Res. 107(D2):ACL 11-1-ACL 11-4
- Otto-Bliesner BL, Upchurch GR. 1997. Vegetation-induced warming of high-latitude regions during the Late Cretaceous period. Nature 385:804-7
- Pearson PN, Ditchfield PW, Singano J, Harcourt-Brown KG, Nicholas CJ, et al. 2001. Warm tropical sea surface temperatures in the Late Cretaceous and Eocene epochs. Nature 413:481-87
- Penn JL, Deutsch C, Payne JL, Sperling EA. 2018. Temperature-dependent hypoxia explains biogeography and severity of end-Permian marine mass extinction. Science 362:eaat1327
- Pincus R, Mlawer EJ, Delamere JS. 2019. Balancing accuracy, efficiency, and flexibility in radiation calculations for dynamical models. J. Adv. Model. Earth Syst. 11:3074-89
- Poulsen CJ, Barron EJ, Peterson WH, Wilson PA. 1999. A reinterpretation of Mid-Cretaceous shallow marine temperatures through model-data comparison. Paleoceanography 14:679–97
- Poulsen CJ, Gendaszek AS, Jacob RL. 2003. Did the rifting of the Atlantic Ocean cause the Cretaceous thermal maximum? Geology 31:115-18
- Poulsen CJ, Tabor C, White JD. 2015. Long-term climate forcing by atmospheric oxygen concentrations. Science 348:1238-41

- Poulsen CJ, Zhou J. 2013. Sensitivity of Arctic climate variability to mean state: insights from the Cretaceous. 7. Clim. 26:7003-22
- Previdi M, Smith KL, Polvani LM. 2021. Arctic amplification of climate change: a review of underlying mechanisms. Environ. Res. Lett. 16:093003
- Rae JWB, Zhang YG, Liu X, Foster GL, Stoll HM, Whiteford RDM. 2021. Atmospheric CO2 over the past 66 million years from marine archives. Annu. Rev. Earth Planet. Sci. 49:609-41
- Reichgelt T, Greenwood DR, Steinig S, Conran JG, Hutchinson DK, et al. 2022. Plant proxy evidence for high rainfall and productivity in the Eocene of Australia. Paleoceanogr. Paleoclimatol. 37:e2022PA004418
- Renoult M, Sagoo N, Zhu J, Mauritsen T. 2023. Causes of the weak emergent constraint on climate sensitivity at the Last Glacial Maximum. Clim. Past 19:323-56
- Rohde RA, Hausfather Z. 2020. The Berkeley Earth land/ocean temperature record. Earth Syst. Sci. Data 12:3469-79
- Russotto RD, Biasutti M. 2020. Polar amplification as an inherent response of a circulating atmosphere: results from the TRACMIP aquaplanets. Geophys. Res. Lett. 47:e2019GL086771
- Sagoo N, Valdes P, Flecker R, Gregoire LJ. 2013. The Early Eocene equable climate problem: Can perturbations of climate model parameters identify possible solutions? Philos. Trans. R. Soc. A 371:20130123
- Schneider T, Kaul CM, Pressel KG. 2019. Possible climate transitions from breakup of stratocumulus decks under greenhouse warming. Nat. Geosci. 12:163-67
- Schneider T, Teixeira J, Bretherton CS, Brient F, Pressel KG, et al. 2017. Climate goals and computing the future of clouds. Nat. Clim. Change 7:3-5
- Schrag DP. 1999. Effects of diagenesis on the isotopic record of late Paleogene tropical sea surface temperatures. Chem. Geol. 161:215-24
- Seeley JT, Jeevanjee N. 2021. H₂O windows and co₂ radiator fins: a clear-sky explanation for the peak in equilibrium climate sensitivity. Geophys. Res. Lett. 48:e2020GL089609
- Seeley JT, Wordsworth RD. 2021. Episodic deluges in simulated hothouse climates. Nature 599:74-79
- Shackleton N, Boersma A. 1981. The climate of the Eocene ocean. J. Geol. Soc. 138:153-57
- Shellito CJ, Lamarque JF, Sloan Lisa C. 2009. Early Eocene Arctic climate sensitivity to pCO₂ and basin geography. Geophys. Res. Lett. 36:L09707
- Sherwood SC, Webb MJ, Annan JD, Armour KC, Forster PM, et al. 2020. An assessment of Earth's climate sensitivity using multiple lines of evidence. Rev. Geophys. 58:e2019RG000678
- Sloan LC, Pollard D. 1998. Polar stratospheric clouds: a high latitude warming mechanism in an ancient greenhouse world. Geophys. Res. Lett. 25:3517-20
- Sriver RL, Huber M. 2007. Observational evidence for an ocean heat pump induced by tropical cyclones. Nature 447:577-80
- Suan G, Popescu S-M, Suc J-P, Schnyder J, Fauquette S, et al. 2017. Subtropical climate conditions and mangrove growth in Arctic Siberia during the early Eocene. Geology 45:539-42
- Tabor CR, Poulsen CJ, Lunt DJ, Rosenbloom NA, Otto-Bliesner BL, et al. 2016. The cause of Late Cretaceous cooling: a multimodel-proxy comparison. Geology 44:963-66
- Thomas DJ, Korty R, Huber M, Schubert JA, Haines B. 2014. Nd isotopic structure of the Pacific Ocean 70-30 Ma and numerical evidence for vigorous ocean circulation and ocean heat transport in a greenhouse world. Paleoceanography 29:454-69
- Tierney JE, Poulsen CJ, Montañez IP, Bhattacharya T, Feng R, et al. 2020. Past climates inform our future. Science 370:eaay3701
- Tierney JE, Zhu J, Li M, Ridgwell A, Hakim GJ, et al. 2022. Spatial patterns of climate change across the Paleocene-Eocene Thermal Maximum. PNAS 119:e2205326119
- Tripati AK, Delaney ML, Zachos JC, Anderson LD, Kelly DC, Elderfield H. 2003. Tropical sea-surface temperature reconstruction for the early Paleogene using Mg/Ca ratios of planktonic foraminifera. Paleoceanography 18:1101
- Vallis GK. 2000. Large-scale circulation and production of stratification: effects of wind, geometry, and diffusion. J. Phys. Oceanogr. 30:933-54
- van Dijk J, Fernandez A, Bernasconi SM, Caves Rugenstein JK, Passey SR, White T. 2020. Spatial pattern of super-greenhouse warmth controlled by elevated specific humidity. Nat. Geosci. 13:739-44

- West CK, Greenwood DR, Reichgelt T, Lowe AJ, Vachon JM, Basinger JF. 2020. Paleobotanical proxies for early Eocene climates and ecosystems in northern North America from middle to high latitudes. Clim. Past 16(4):1387-410
- Westerhold T, Marwan N, Drury AJ, Liebrand D, Agnini C, et al. 2020. An astronomically dated record of Earth's climate and its predictability over the last 66 million years. Science 369:1383-87
- Wilson PA, Norris RD, Cooper MJ. 2002. Testing the Cretaceous greenhouse hypothesis using glassy foraminiferal calcite from the core of the Turonian tropics on Demerara Rise. Geology 30:607-10
- Zachos JC, Stott LD, Lohmann KC. 1994. Evolution of Early Cenozoic marine temperatures. Paleoceanography 9:353-87
- Zhang Y, de Boer AM, Lunt DJ, Hutchinson DK, Ross P, et al. 2022. Early Eocene ocean meridional overturning circulation: the roles of atmospheric forcing and strait geometry. Paleoceanogr. Paleoclimatol. 37:e2021PA004329
- Zhu J, Otto-Bliesner BL, Brady EC, Gettelman A, Bacmeister JT, et al. 2022. LGM paleoclimate constraints inform cloud parameterizations and equilibrium climate sensitivity in CESM2. J. Adv. Model. Earth Syst. 14:e2021MS002776
- Zhu J, Otto-Bliesner BL, Brady EC, Poulsen CJ, Tierney JE, et al. 2021. Assessment of equilibrium climate sensitivity of the Community Earth System Model Version 2 through simulation of the Last Glacial Maximum. Geophys. Res. Lett. 48:e2020GL091220
- Zhu J, Poulsen CJ. 2020. On the increase of climate sensitivity and cloud feedback with warming in the community atmosphere models. Geophys. Res. Lett. 47:e2020GL089143
- Zhu J, Poulsen CJ, Otto-Bliesner BL. 2020a. High climate sensitivity in CMIP6 model not supported by paleoclimate. Nat. Clim. Change 10:378-79
- Zhu J, Poulsen CJ, Otto-Bliesner BL, Liu Z, Brady EC, Noone DC. 2020b. Simulation of early Eocene water isotopes using an Earth system model and its implication for past climate reconstruction. Earth Planet. Sci. Lett. 537:116164
- Zhu J, Poulsen CJ, Tierney JE. 2019. Simulation of Eocene extreme warmth and high climate sensitivity through cloud feedbacks. Sci. Adv. 5:eaax1874